

# Geometric Methods for Sampling, Optimisation, Inference and Adaptive Agents

Alessandro Barp<sup>1,2,†</sup>, Lancelot Da Costa<sup>3,4,†</sup>, Guilherme França<sup>5,†</sup>, Karl Friston<sup>4</sup>,  
Mark Girolami<sup>1,2</sup>, Michael I. Jordan<sup>5,6</sup>, and Grigorios A. Pavliotis<sup>3</sup>

<sup>1</sup>*Department of Engineering, University of Cambridge, Cambridge, UK*

<sup>2</sup>*The Alan Turing Institute, The British Library, London, UK*

<sup>3</sup>*Department of Mathematics, Imperial College London, London, UK*

<sup>4</sup>*Wellcome Centre for Human Neuroimaging, University College London, London, UK*

<sup>5</sup>*Computer Science Division, University of California, Berkeley, USA*

<sup>6</sup>*Department of Statistics, University of California, Berkeley, USA*

<sup>†</sup>Equal contribution

## Abstract

In this chapter, we identify fundamental geometric structures that underlie the problems of sampling, optimisation, inference and adaptive decision-making. Based on this identification, we derive algorithms that exploit these geometric structures to solve these problems efficiently. We show that a wide range of geometric theories emerge naturally in these fields, ranging from measure-preserving processes, information divergences, Poisson geometry, and geometric integration. Specifically, we explain how *(i)* leveraging the symplectic geometry of Hamiltonian systems enable us to construct (accelerated) sampling and optimisation methods, *(ii)* the theory of Hilbertian subspaces and Stein operators provides a general methodology to obtain robust estimators, *(iii)* preserving the information geometry of decision-making yields adaptive agents that perform active inference. Throughout, we emphasise the rich connections between these fields; e.g., inference draws on sampling and optimisation, and adaptive decision-making assesses decisions by inferring their counterfactual consequences. Our exposition provides a conceptual overview of underlying ideas, rather than a technical discussion, which can be found in the references herein.

*Keywords:* information geometry; Hamiltonian Monte Carlo; Stein’s method; reproducing kernel; variational inference; accelerated optimisation; dissipative systems; decision theory; active inference.

# Contents

<b>1</b>	<b>Introduction</b>	<b>2</b>
<b>2</b>	<b>Accelerated optimisation</b>	<b>4</b>
2.1	Principle of geometric integration . . . . .	4
2.2	Conservative flows and symplectic integrators . . . . .	5
2.3	Rate-matching integrators for smooth optimisation . . . . .	7
2.4	Manifold and constrained optimisation . . . . .	10
2.5	Gradient flow as a high friction limit . . . . .	11
2.6	Optimisation on the space of probability measures . . . . .	12
<b>3</b>	<b>Hamiltonian-based accelerated sampling</b>	<b>13</b>
3.1	Optimising diffusion processes for sampling . . . . .	14
3.2	Hamiltonian Monte Carlo . . . . .	16
<b>4</b>	<b>Statistical inference with kernel-based discrepancies</b>	<b>19</b>
4.1	Topological methods for MMDs . . . . .	20
4.2	Smooth measures and KSDs . . . . .	21
4.2.1	The canonical Stein operator and Poincaré duality . . . . .	21
4.2.2	Kernel Stein discrepancies and score matching . . . . .	23
4.3	Information geometry of MMDs and natural gradient descent . . . . .	24
4.3.1	Minimum Stein discrepancy estimators . . . . .	24
4.3.2	Likelihood-free inference with generative models . . . . .	25
<b>5</b>	<b>Adaptive agents through active inference</b>	<b>25</b>
5.1	Modelling adaptive decision-making . . . . .	26
5.1.1	Behaviour, agents and environments . . . . .	26
5.1.2	Decision-making in precise agents . . . . .	26
5.1.3	The information geometry of decision-making . . . . .	27
5.2	Realising adaptive agents . . . . .	29
5.2.1	The basic active inference algorithm . . . . .	29
5.2.2	Sequential decision-making under uncertainty . . . . .	30
5.2.3	World model learning as inference . . . . .	30
5.2.4	Scaling active inference . . . . .	32

## 1 Introduction

Differential geometry plays a fundamental role in applied mathematics, statistics, and computer science, including numerical integration [1–5], optimisation [6–11], sampling [12–16], statistics on spaces with deep learning [17, 18], medical imaging and shape methods [19, 20], interpolation [21], and the study of random maps [22], to name a few. Of particular relevance to this chapter is information geometry, i.e., the differential geometric treatment of smooth statistical manifolds, whose origin stems from a seminal article by Rao [23] who introduced the Fisher metric tensor on parametrised statistical models, and thus a natural Riemannian geometry that was later observed to correspond to an infinitesimal distance with respect to the Kullback–Leibler (KL) divergence [24]. The geometric study of statistical models has had many successes [25–27], ranging from statistical inference, where it was used to prove the optimality of the maximum likelihood estimator [28], to

the construction of the category of mathematical statistics, generated by Markov morphisms [29,30]. Our goal in this chapter is to discuss the emergence of natural geometries within a few important areas of statistics and applied mathematics, namely *optimisation*, *sampling*, *inference*, and *adaptive agents*. We provide a conceptual introduction to the underlying ideas rather than a technical discussion, highlighting connections with various fields of mathematics and physics.

The vast majority of statistics and machine learning applications involve solving *optimisation* problems. Accelerated gradient-based methods [31,32], and several variations thereof, have become workhorses in these fields. Recently, there has been great interest in studying such methods from a continuous-time limiting perspective; see, e.g., [33–40] and references therein. Such methods can be seen as 1st order integrators to a classical *Hamiltonian system with dissipation*. This raises the question on how to discretise the system such that important properties are preserved, assuming the system has fast convergence to critical points and desirable stability properties. It has been known for a long time that the class of *symplectic integrators* is the preferred choice for simulating physical systems [1,2,41–48]. These discretisation techniques, designed to preserve the underlying (symplectic) geometry of Hamiltonian systems, also form the basis of *Hamiltonian Monte Carlo* (HMC) (or hybrid Monte Carlo) methods [13,49]. Originally, such a theory of geometric integration was developed with conservative systems in mind while, in optimisation, the associated system is naturally a dissipative one. Nevertheless, symplectic integrators were exploited in this context [6–8]. More recently, it has been proved that a generalisation of symplectic integrators to dissipative Hamiltonian systems is indeed able to preserve rates of convergence and stability [9], which are the main properties of interest for optimisation. Followup work [10] extended this approach, enabling optimisation on *manifolds* and problems with *constraints*. There is also a tight connection between optimisation on the space of measures and sampling which dates back to [50,51]; we will revisit these ideas in relation to dissipative Hamiltonian systems.

*Sampling* methods are critical to the efficient implementation of many methodologies. Most modern samplers are based on Markov Chain Monte Carlo methods, which include slice samplers [52,53], piecewise-deterministic Markov chains, such as bouncy particle and zig-zag samplers [54–59], Langevin algorithms [60–62], interacting particle systems [63] and the class of HMC methods [12–14,49,64,65]. The original HMC algorithm was introduced in physics to sample distributions on gauge groups for lattice quantum chromodynamics [13]. It combined two approaches that emerged in previous decades, namely the Metropolis-Hastings algorithm and the Hamiltonian formulation of molecular dynamics [66–68]. Modern HMC relies heavily on symplectic integrators to simulate a deterministic dynamic, responsible for generating distant moves between samples and thus reduce their correlation, while at the same time preserving important geometric properties. This deterministic step is then usually combined with a corrective step (originally a Metropolis-Hastings acceptance step) to ensure preservation of the correct target, and with a stochastic process, employed to speed up convergence to the target distribution. We will first focus on the geometry of measure-preserving diffusions, which emerges from ideas formulated by Poincaré and Volterra, and form the building block of many samplers. In particular, we will discuss ways to “accelerate” sampling using irreversibility and hypoellipticity. We will then introduce HMC focusing on its underlying Poisson geometry, the important role played by symmetries, and its connection to geometric integration.

We then discuss the problem of *statistical inference*, whose practical implementation usually relies upon sampling and optimisation. Given observations from a target distribution, many estimators belong to the family of the so-called  $M$  and  $Z$  estimators [69], which are obtained by finding the parameters that maximises (or are zeros of) a parametrised set of functions. These include the maximum likelihood and minimum Hyvärinen score matching estimators [70,71], which are also particular instances of the minimum score estimators induced by scoring rules that quantify

the discrepancy between a sample and a distribution [72]. The Monge–Kantorovich transportation problem [73] motivates another important class of estimators, namely the minimum Kantorovich and  $p$ -Wasserstein estimators, whose implementation use the Sinkhorn discrepancy [74–76]. Our discussion of inference builds upon the theory of Hilbertian subspaces and, in particular, reproducing kernels. These inference schemes rely on the continuity of linear functionals, such as probability and Schwartz distributions, over a class of functions to geometrize the analysis of integral probability metrics which measure the worst case integration error. We shall explain how maximum mean, kernelised, and score matching discrepancies arise naturally from topological considerations.

Models of *adaptive agents* are the basis of algorithmic-decision-making under uncertainty. This is a difficult problem that spans multiple disciplines such as statistical decision theory [77], game theory [78], control theory [79], reinforcement learning [80], and active inference [81]. To illustrate a generic use case for the previous methodologies we consider active inference, a unifying formulation of behaviour—subsuming perception, planning and learning—as a process of inference [81–84]. We describe decision-making under active inference using information geometry, revealing several special cases that are established notions in statistics, cognitive science and engineering. We then show how preserving this information geometry in algorithms enables adaptive algorithmic decision-making, endowing robots and artificial agents with useful capabilities, including robustness, generalisation and context-sensitivity [85, 86]. Active inference is an interesting use case because it has yet to be scaled—to tackle high dimensional problems—to the same extent as established approaches, such as reinforcement learning [87]; however, numerical analyses generally show that active inference performs at least as well in simple environments [88–94], and better in environments featuring volatility, ambiguity and context switches [91, 92].

## 2 Accelerated optimisation

We shall be concerned with the problem of optimisation of a function  $V : \mathcal{M} \rightarrow \mathbb{R}$ , i.e., finding a point that maximises  $V(q)$ , or minimises  $-V(q)$ , over a smooth manifold  $\mathcal{M}$ . We will assume this function is differentiable to construct algorithms that rely on the flows of smooth vector fields guided by the derivatives of  $V(q)$ .

Many algorithms in optimisation are given as a sequence of finite differences, represented by iterations of a mapping  $\Psi_{\delta t} : \mathcal{M} \rightarrow \mathcal{M}$ , where  $\delta t > 0$  is a step size. The analysis of such finite difference iterations is usually challenging, relying on painstaking algebra to obtain theoretical guarantees; such as convergence to a critical point, stability, and rates of convergence to a critical point. Even when these algorithms are seen as discretisations of a continuum system, whose behaviour is presumably understood, it is well-known that most discretisations break important properties of the system.

### 2.1 Principle of geometric integration

Fortunately, here comes into play one of the most fundamental ideas of *geometric integration*: many numerical integrators are very close—exponentially in the step size—to a smooth dynamics generated by a *shadow vector field* (a perturbation of the original vector field). This allows us to analyse the discrete trajectory implemented by the algorithm using powerful tools from dynamical systems and differential geometry, which are a priori reserved to smooth systems. Crucially, while numerical integrators typically diverge significantly from the dynamics they aim to simulate, *geometric integrators* respect the main properties of the system. In the context of optimisation this means respecting stability and rates of convergence. This was first demonstrated in [9] and further extended in [10]; our following discussion will be based on these works.

The simplest way to construct numerical methods to simulate the flow of a vector field  $X$  arises when it is given by a sum,  $X = Y + Z$ , and the flows of the individual vector fields  $Y$  and  $Z$  are—analytically or numerically—tractable. In such a case, we can approximate the exact flow  $\Phi_{\delta t}^X = e^{\delta t X}$ , for step size  $\delta t > 0$ , by composing the individual flows  $\Phi_{\delta t}^Y = e^{\delta t Y}$  and  $\Phi_{\delta t}^Z = e^{\delta t Z}$ . The simplest composition is given by  $\Psi_{\delta t}^X \equiv \Phi_{\delta t}^Y \circ \Phi_{\delta t}^Z$ . The *Baker–Campbell–Hausdorff* (BCH) formula then yields

$$e^{\delta t Y} \circ e^{\delta t Z} = e^{\delta t \tilde{X}}, \quad \tilde{X} = (Y + Z) + \frac{1}{2}[Y, Z]\delta t + \frac{1}{12}([Y, [Y, Z]] - [Z, [Y, Z]])\delta t^2 + \dots, \quad (1)$$

where  $[Y, Z] = YZ - ZY$  is the commutator between  $Y$  and  $Z$ . Thus, the numerical method itself can be seen as a smooth dynamical system with flow map  $\Psi_{\delta t}^X = e^{\delta t \tilde{X}}$ . The goal of *geometric integration* is to construct numerical methods for which  $\tilde{X}$  shares with  $X$  the critical properties of interest; this is usually done by requiring preservation of some geometric structure.

Recall that a numerical map  $\Psi_{\delta t}^X$  is said to be of order  $r \geq 1$  if  $|\Psi_{\delta t}^X - \Phi_{\delta t}^X| = \mathcal{O}(\delta t^{r+1})$ ; we abuse notation slightly and let  $|\cdot|$  denote a well-defined distance over manifolds (see [95] for details). Thus, the expansion (1) also shows that the error in the approximation is  $|\Psi_{\delta t}^X - \Phi_{\delta t}^X| = \mathcal{O}(\delta t^2)$ , i.e., we have an integrator of order  $r = 1$ . One can also consider more elaborate compositions, such as

$$\Psi_{\delta t}^X \equiv \Phi_{\delta t/2}^Y \circ \Phi_{\delta t}^Z \circ \Phi_{\delta t/2}^Y, \quad (2)$$

which is more accurate since the first term in (1) cancels out, yielding an integrator of order  $r = 2$ .<sup>1</sup>

## 2.2 Conservative flows and symplectic integrators

As a stepping stone, we first discuss the construction of suitable *conservative flows*, namely flows along which some function  $f : \mathcal{X} \rightarrow \mathbb{R}$  is constant, where  $\mathcal{X}$  is the phase space manifold of the system, i.e., the space in which the dynamics evolves. Such flows, which are amongst the most well-studied due to their importance in physics, will enable us to obtain our desired “rate-matching” optimisation methods and will also be central in our construction of geometric samplers.

To construct vector fields along the derivative of  $f$  we shall need *brackets*. Geometrically, these are morphisms  $\mathcal{X}^* \rightarrow \mathcal{X}$ , also known as contravariant tensors of rank 2 in physics, where  $\mathcal{X}^*$  is the dual space of  $\mathcal{X}$ . Note that on Riemannian manifolds (e.g.,  $\mathcal{X} = \mathbb{R}^n$ ) both spaces are isomorphic. In Euclidean space,  $x \in \mathcal{X} = \mathbb{R}^n$ , we define such  $B$ -vector fields in terms of a state-dependent matrix  $B = B(x)$  as<sup>2</sup>

$$X_f^B(x) \equiv B^{ij}(x)\partial_i f(x)\partial_j. \quad (3)$$

Any vector field that depends linearly and locally on  $f$  may be written in this manner. Notice that a decomposition  $f = \sum_a f_a$  induces a decomposition  $X_f^B = \sum_a X_{f_a}^B$  that is amenable to the splitting integrators previously mentioned. Importantly, vector fields that preserve  $f$  correspond to *bracket vector fields* in which  $B$  is *antisymmetric* [96]. Constructing conservative flows is thus straightforward. Unfortunately, it is a rather more challenging task to construct efficient discretisations that retain this property; most well-known procedures, namely discrete-gradient and projection methods, only give rise to integrators that require solving implicit equations at every step, and they may break other important properties of the system.

<sup>1</sup>Higher-order methods are constructed by looking for appropriate compositions that cancel first terms in the BCH formula [43]. However, methods for  $r > 2$  tend to be expensive numerically, with not so many benefits (if any) over methods of order  $r = 2$ .

<sup>2</sup>We denote by  $x^i$  the  $i$ th component of  $x$  and  $\partial_i \equiv \partial/\partial x^i$ . We also use Einstein’s summation convention, i.e., repeated upper and lower indices are summed over.

For a particular class of conservative flows, it is possible to construct splitting integrators that—exactly—preserve another function  $\tilde{f}$  that remains close to  $f$ . Indeed, going back to the BCH formula (1), we see that if we were to approximate a conservative flow of  $X_f^B = X_{f_1}^B + X_{f_2}^B$  by composing the flows of  $X_{f_1}^B$  and  $X_{f_2}^B$ , and, crucially, if we had a bracket for which the commutators can be written as

$$[X_{f_1}^B, X_{f_2}^B] = X_{f_3}^B,$$

for some function  $f_3$ , and so on for all commutators in (1), then the right-hand side of the BCH formula would itself be an expansion in terms of a vector field  $X_{\tilde{f}}^B$  for some *shadow function*  $\tilde{f} = f + f_3\delta t + f_4\delta t^2 + \dots$ . In particular,  $\tilde{f}$  would inherit all the properties of  $f$ , i.e., properties common to  $B$ -vector fields. This is precisely the case for *Poisson brackets*, written  $B \equiv \Pi$ , which are antisymmetric brackets for which the Jacobi identity holds:

$$[X_f^\Pi, X_g^\Pi] = X_{\{f,g\}}^\Pi, \quad \{f,g\} \equiv \partial_i f \Pi^{ij} \partial_j g, \quad (4)$$

where  $\{f,g\}$  is the Poisson bracket between functions  $f$  and  $g$ . The BCH formula then implies

$$\tilde{f} = (f_1 + f_2) + \frac{1}{2}\{f_1, f_2\}\delta t + \frac{1}{12}(\{f_1, \{f_1, f_2\}\} + \{f_2, \{f_2, f_1\}\})\delta t^2 + \dots \quad (5)$$

Such an integrator can thus be seen as a Poisson system itself, generated by the above asymptotic shadow  $\tilde{f}$ , which is exactly preserved.

Poisson brackets and their dynamics are the most important class of conservative dynamical systems, describing many physical systems, including all of fluid and classical mechanics. The two main classes of Poisson brackets are constant antisymmetric matrices on Euclidean space, and *symplectic brackets* for which  $\Pi^{ij}(x)$  is invertible at every point  $x$ . Its inverse is denoted by  $\Omega_{ij} = (\Pi^{-1})_{ij}$  and called a *symplectic form*. In this case, the function  $f$  is called a Hamiltonian, denoted  $f = H$ . The invertibility of the Poisson tensor  $\Pi^{ij}$  implies that such a bracket exists only on *even-dimensional spaces*. Darboux theorem then ensures the existence of local coordinates  $x \equiv (q^1, \dots, q^d, p_1, \dots, p_d)$  in which the symplectic form can be represented as  $\Omega = \begin{pmatrix} 0 & I \\ -I & 0 \end{pmatrix}$ . Dynamically, this corresponds to the fact that these are 2nd order differential equations, requiring not only a position  $q \in \mathcal{M}$  but also a momentum  $p \in T_q^* \mathcal{M}$ .<sup>3</sup> Note that if  $H = p_i$  then  $X_H = \partial/\partial q^i$ , and conversely if  $H = q^i$  then  $X_H = -\partial/\partial p_i$ . Thus, a change in coordinate  $q^i$  is generated by its conjugate momentum  $p_i$ , and vice-versa. Thus, the only way to generate dynamics on  $\mathcal{M}$  in this case is by introducing a Hamiltonian depending on both position and momentum. From a numerical viewpoint, the extended phase space introduces extra degrees of freedom that allow us to incorporate “symmetries” in the Hamiltonian, which facilitate integration. Indeed, in practice, the Hamiltonian usually decomposes into a potential energy, associated to position and independent of momentum, and a kinetic energy, associated to momentum and invariant under position changes, both generating tractable flows. Thanks to this decomposition, we are able to construct numerical methods through splitting the vector field. Note also that, for symplectic brackets, the existence of a shadow Hamiltonian can be guaranteed beyond the case of splitting methods, e.g., for variational integrators—which use a discrete version of Hamilton’s principle of least action—and more generally for most symplectic integrators in which the symplectic bracket is preserved up to topological considerations described by the 1st de Rham cohomology of phase space.

---

<sup>3</sup>More precisely, the dynamics evolve on the cotangent bundle  $\mathcal{X} = T^* \mathcal{M}$ , with coordinates  $x = (q, p)$ ; momentum  $p \in T_q^* \mathcal{M}$  and velocity  $v = dq/dt \in T_q \mathcal{M}$  are equivalent on the Riemannian manifolds that are used in practice.  $\mathcal{M}$  is called the configuration manifold with coordinates  $q$ .

### 2.3 Rate-matching integrators for smooth optimisation

Having obtained a vast family of smooth dynamics and integrators that closely preserve  $f$ , we can now apply these ideas to optimisation. Vector fields for which a Hamiltonian function  $f = H$  *dissipates* can be written as a bracket vector field  $X_H^B$  for some negative semi-definite matrix  $B$  [96]. Let us consider a concrete example in  $\mathcal{X} = \mathbb{R}^{2d}$  in the form of a (generalised) *conformal Hamiltonian system* [8, 9, 97]. Consider thus the Hamiltonian

$$H(q, p) = \frac{1}{2} p_i g^{ij} p_j + V(q), \quad (6)$$

where  $g_{ij}$  is a constant *symmetric positive definite* matrix with inverse  $g^{ij}$ . The associated vector field is  $X_H^B = g^{ij} p_j \partial_{q^i} - [\partial_{q^i} V + \gamma(t) p_i] \partial_{p_i}$ , with  $\gamma(t) > 0$  being a “damping coefficient.” This is associated to the *negative definite matrix*

$$B \equiv \underbrace{\begin{pmatrix} 0 & -I \\ I & 0 \end{pmatrix}}_{\text{conservative}} - \underbrace{\gamma(t) \begin{pmatrix} 0 & 0 \\ 0 & I \end{pmatrix}}_{\text{dissipative}}. \quad (7)$$

The equations of motion are

$$\frac{dq^i}{dt} = g^{ij} p_j, \quad \frac{dp_i}{dt} = -\frac{\partial V}{\partial q^i} - \gamma(t) p_i, \quad (8)$$

and obey

$$\frac{dH}{dt} = -\gamma(t) p_i g^{ij} p_j \leq 0, \quad (9)$$

so the system is *dissipative*. Suppose  $V(q)$  has a minimizer  $q^* \equiv \arg \min_q V(q)$  in some region of interest and, without loss of generality, has value  $V^* \equiv V(q^*) \equiv 0$ . Then  $H > 0$  and  $dH/dt < 0$  outside such a critical point, implying that  $H$  is also a (strict) *Lyapunov function*; the existence of such a Lyapunov function implies that trajectories starting in the neighborhood of  $q^*$  will converge to  $q^*$ . In other words, the above system provably solves the optimisation problem

$$\min_{q \in \mathbb{R}^d} V(q). \quad (10)$$

Two common choices for the damping are the constant case,  $\gamma(t) = \gamma$ , and the asymptotic vanishing case,  $\gamma(t) = r/t$  for some constant  $r \geq 3$  (other choices are also possible). When  $V(q)$  is a convex function (resp. strongly convex function with parameter  $\mu > 0$ ) it is possible to show the following convergence rates [37]:

	<i>convex</i>	<i><math>\mu</math>-strongly convex</i>	<i>damping</i>	
$V(q(t)) - V^*$	$\mathcal{O}(t^{-1})$	$\mathcal{O}(\exp\{-\sqrt{\mu/\lambda_1^2(g)}t\})$	$\gamma(t) = \text{const.}$	(11)
	$\mathcal{O}(\lambda_1^2(g)t^{-2})$	$\mathcal{O}(t^{-2r/3})$	$\gamma(t) = r/t$	

where  $\lambda_1(g)$  is the largest eigenvalue of the metric  $g$ . The *convergence rates* of this system are therefore known under such convexity assumptions. Ideally, we want to design optimisation methods that preserve these rates, i.e., are “rate-matching”, and are also numerically stable. As we will see, such geometric integrators can be constructed by leveraging the shadow Hamiltonian property of

symplectic methods on higher-dimensional conservative Hamiltonian systems [9] (see also [98, 99]). This holds not only on  $\mathbb{R}^{2d}$  but on general settings, namely on arbitrary smooth manifolds [9, 10].

In the conformal Hamiltonian case, the dissipation appears explicitly in the equations of motion. It is however theoretically convenient to consider an equivalent *explicit time-dependent* Hamiltonian formulation. Consider the following coordinate transformation into system (8):

$$p \mapsto e^{-\eta(t)}p, \quad H(q, p) \mapsto e^{\eta(t)}H(q, e^{-\eta(t)}p), \quad \eta(t) \equiv \int \gamma(t)dt. \quad (12)$$

It is easy to see that (8) is equivalent to standard Hamilton's equations,

$$\frac{dq^i}{dt} = \frac{\partial H}{\partial p_i}, \quad \frac{dp_i}{dt} = -\frac{\partial H}{\partial q^i},$$

with the explicit time-dependent Hamiltonian

$$H(t, q, p) = \frac{1}{2}e^{-\eta(t)}p_i g^{ij} p_j + e^{\eta(t)}V(q). \quad (13)$$

The rate of change of  $H$  along the flow now satisfies

$$\frac{dH}{dt} = \frac{\partial H}{\partial t} \neq 0, \quad (14)$$

so the system is *nonconservative*; this equation is equivalent to (9).

Going one step further, let us now promote  $t$  to a new coordinate and introduce its (conjugate) momentum  $u$ . Consider thus the higher-dimensional Hamiltonian

$$K(t, q, u, p) \equiv \frac{1}{2}e^{-\eta(t)}p_i g^{ij} p_j + e^{\eta(t)}V(q) + u. \quad (15)$$

Note that  $t$  and  $u$  are two arbitrary canonical coordinates. Denoting the time parameter of this system by  $s$ , Hamilton's equations read

$$\frac{dt}{ds} = 1, \quad \frac{du}{ds} = -\frac{\partial K}{\partial t}, \quad \frac{dq^i}{ds} = e^{-\eta(t)}g^{ij}p_j, \quad \frac{dp_i}{ds} = -e^{\eta(t)}\frac{\partial V}{\partial q^i}. \quad (16)$$

This system is *conservative* since  $dK/ds = 0$ . Now, if we fix coordinates as

$$t = s, \quad u(s) = -H(s, q(s), p(s)), \quad (17)$$

the conservative system (16) reduces precisely the original dissipative system (13); the 2nd equation in (16) reproduces (14), and the remaining equations are equivalent to the equations of motion associated to (13), which in turn are equivalent to (8) as previously noted. Formally, what we have done is to embed the original dissipative system with phase space  $\mathbb{R}^{2d}$  into a higher-dimensional conservative system with phase space  $\mathbb{R}^{2d+2}$ . The dissipative dynamics thus lies on a hypersurface of constant energy,  $K = 0$ , in high dimensions; see [9] for details. The reason for doing this procedure, *called symplectification*, is purely theoretical: since the theory of symplectic integrators only accounts for conservative systems, we can now extend this theory to dissipative settings by applying a symplectic integrator to (13) and then fixing the relevant coordinates (17) in the resulting method. Geometrically, this corresponds to integrating the time flow exactly [9, 98]. In [9] such a procedure was defined under the name of *presymplectic integrators*, and these connections hold not only for the specific example above but also for general non-conservative Hamiltonian systems.



We are now ready to explain why this approach is suitable to construct practical optimisation methods. Let  $\Psi_{\delta s} : \mathbb{R}^{2d+2} \rightarrow \mathbb{R}^{2d+2}$  be a symplectic integrator of order  $r \geq 1$  applied to system (15). Denote by  $(t_k, q_k, u_k, p_k)$  the numerical state, obtained by  $k = 0, 1, \dots$  iterations of  $\Psi_{\delta s}$ . Time is simulated over the grid  $s_k = (\delta s)k$ , with step size  $\delta t > 0$ . Because a symplectic integrator has a shadow Hamiltonian we have

$$\tilde{K}(t_k, q_k, u_k, p_k) = K(t(s_k), q(s_k), u(s_k), p(s_k)) + \mathcal{O}(\delta s^r).$$

Enforcing (17), the coordinate  $t_k$  becomes simply the time discretization  $s_k$ , which is exact, and so is  $u_k = u(t_k)$  since it is a function of time alone; importantly,  $u$  does not couple to any of the other degrees of freedom so it is irrelevant whether we have access to  $u(s)$  or not. Replacing (15) into the above equation we conclude:

$$\tilde{H}(t_k, q_k, p_k) = H(t_k, q(t_k), p(t_k)) + \mathcal{O}(\delta t^r), \quad (18)$$

where we now denote  $t_k = (\delta t)k$ , for  $k = 0, 1, \dots$ . Hence, the time-dependent Hamiltonian also has a shadow, thanks to the cancellation of the variable  $u$ . In particular, if we replace the explicit form of the Hamiltonian (13) we obtain<sup>4</sup>

$$\underbrace{V(q_k) - V^*}_{\text{numerical rate}} = \underbrace{V(q(t_k)) - V^*}_{\text{continuum rate}} + \underbrace{\mathcal{O}(e^{-\eta(t_k)}\delta t^r)}_{\text{small error}}. \quad (19)$$

Therefore, the known rates (11) for the continuum system are nearly preserved—and so would be any rates of more general time-dependent (dissipative) Hamiltonian systems. Moreover, as a consequence of (18), the original time-independent Hamiltonian (6) of the conformal formulation is also closely preserved, i.e., within the same *bounded error* in  $\delta t$ —recall transformation (12). However, this is also a Lyapunov function, hence the numerical method respects the *stability properties* of the original system as well.<sup>5</sup>

In short, as a consequence of having a shadow Hamiltonian, such geometric integrators are able to reproduce all the relevant properties of the continuum system. These arguments are completely general; namely, they ultimately rely on the BCH formula, the existence of bracket vector fields and the symplectification procedure. Under these basic principles, no discrete-time analyses were necessary to obtain guarantees for the numerical method; which may not be particularly enlightening from a dynamical systems viewpoint and are only applicable on a (painful) case-by-case basis.

Let us now present an explicit algorithm to solve the optimisation problem (10). Consider a generic (conservative) Hamiltonian  $H(q, p)$ , evolving in time  $s$ . The well-known *leapfrog* or Störmer-Verlet method, the most used symplectic integrator in the literature, is based on the composition (2) and reads [2]

$$\begin{aligned} p_{k+1/2} &= p_k - (\delta s/2)\partial_q H(q_k, p_{k+1/2}), \\ q_{k+1} &= q_k - (\delta s/2) [\partial_p H(q_k, p_{k+1/2}) + \partial_p H(q_{k+1}, p_{k+1/2})], \\ p_{k+1} &= p_{k+1/2} - (\delta s/2)\partial_q H(q_{k+1}, p_{k+1/2}). \end{aligned}$$

<sup>4</sup>The kinetic part only contributes to the small error since  $g$  is positive definite and  $|p_k - p(t_k)| = \mathcal{O}(\delta t^r)$ . There are several technical details we are omitting, such as Lipschitz conditions on the Hamiltonian and on the numerical method, which we refer to [9] for details.

<sup>5</sup>Naturally, all these results hold for suitable choices of step size, which can be determined by a linear stability analysis of the particular numerical method under consideration.

According to our prescription, replacing the higher-dimensional Hamiltonian (15), imposing the gauge fixing conditions (17), and recalling that  $u$  cancels out, we obtain the following method:<sup>6</sup>

$$\begin{aligned} p_{k+1/2} &= p_k - (\delta t/2)e^{\eta(t_k)}\partial_q V(q_k), \\ q_{k+1} &= q_k - (\delta t/2)[e^{-\eta(t_k)} + e^{-\eta(t_{k+1})}]g^{-1}p_{k+1/2}, \\ p_{k+1} &= p_{k+1/2} - (\delta t/2)e^{\eta(t_{k+1})}\partial_q V(q_{k+1}), \end{aligned} \tag{20}$$

where we recall that  $\delta t > 0$  is the step size and  $t_k = (\delta t)k$ , for iterations  $k = 0, 1, \dots$ . This method, which is a dissipative generalisation of the leapfrog, was proposed in [9] and has very good performance when solving unconstrained problems (10). In a similar fashion, one can extend any (known) symplectic integrator to a dissipative setting; the above method is just one such example.

## 2.4 Manifold and constrained optimisation

Following [10], we briefly mention how the previous approach can be extended in great generality, i.e., to an optimisation problem

$$\min_{q \in \mathcal{M}} V(q), \tag{21}$$

where  $\mathcal{M}$  is an arbitrary Riemannian manifold. There are essentially two ways to solve this problem through a (dissipative) Hamiltonian approach. One is to simulate a Hamiltonian dynamics on  $T^*\mathcal{M}$  by incorporating the metric of  $\mathcal{M}$  in the kinetic part of the Hamiltonian. Another is to consider a Hamiltonian dynamics on  $\mathbb{R}^n$  and embed  $\mathcal{M}$  into  $\mathbb{R}^n$  by imposing several constraints,<sup>7</sup>

$$\psi_a(q) = 0, \quad a = 1, \dots, m. \tag{22}$$

This constrained case turns out to be particularly useful since we typically are unable to compute the geodesic flow on  $\mathcal{M}$ , but are able to construct robust constrained symplectic integrators for it.

As an example of the first approach, consider  $\mathcal{M} = \mathcal{G}$  being a *Lie group*, with Lie algebra  $\mathfrak{g}$  and generators  $\{T_i\}$ . The analogous of Hamiltonian (13) is given by  $H = -\frac{1}{4g}e^{-\eta(t)}\text{Tr}(P^2) + e^{\eta(t)}V(Q)$ , where  $g > 0$  is a constant,  $Q \in \mathcal{G}$  and  $P \in \mathfrak{g}$  (they can be seen as matrices). The method (20) can be adapted to this setting, resulting in the following algorithm [10] (recall footnote 6):

$$\begin{aligned} P_{k+1/2} &= e^{-\Delta\eta_k} \{P_k - (\delta t/2)\text{Tr}[\partial_Q V(Q_k) \cdot Q_k \cdot P_k] P_k\}, \\ Q_{k+1} &= Q_k \exp[\delta t \cosh(\Delta\eta_k)g^{-1}P_{k+1/2}], \\ P_{k+1} &= e^{-\Delta\eta_k} P_{k+1/2} - (\delta t/2)\text{Tr}[\partial_Q V(Q_{k+1}) \cdot Q_{k+1} \cdot P_{k+1/2}] P_k, \end{aligned} \tag{23}$$

---

<sup>6</sup> In a practical implementation, it is convenient to make the change of variables  $p_k \mapsto e^{\eta(t_k)}p_k$  into (20); recall the transformations (12). In this case the method reads

$$\begin{aligned} p_{k+1/2} &= e^{-\Delta\eta_k} [p_k - (\delta t/2)\partial_q V(q_k)], \\ q_{k+1} &= q_k - \delta t \cosh(\Delta\eta_k)g^{-1}p_{k+1/2}, \\ p_{k+1} &= e^{-\Delta\eta_k} p_{k+1/2} - (\delta t/2)\partial_q V(q_{k+1}), \end{aligned}$$

where  $\Delta\eta_k \equiv \eta(t_{k+1/2}) - \eta(t_k) = \int_{t_k}^{t_{k+1/2}} \gamma(t)dt$ . Note that only a half-step difference of  $\eta(t)$  appears in these updates. The algorithm is thus written in the same variables as the conformal representation (8). The advantage is that we do not have large or small exponentials, which can be problematic numerically. Furthermore, when solving optimisation problems, it is convenient to set the matrix  $g = (\delta t)I$ ; this was noted in [8] but can also be understood from the rates (11) since then the step size  $\delta t$  disappears from some of these formulas.

<sup>7</sup>Theoretically, there is no loss of generality since Nash or Whitney embedding theorems tells us that any smooth manifold  $\mathcal{M}$  can be embedded into  $\mathbb{R}^n$  for sufficiently large  $n$ .

where  $(\partial_Q V(Q))_{ij} = \partial V / \partial Q_{ji}$  is a matrix.

As an example of the second approach, one can constrain the integrator on  $\mathbb{R}^n$  to define a symplectic integrator on  $\mathcal{M}$  via the discrete constrained variational approach [5] by introducing Lagrange multipliers, i.e., by considering the Hamiltonian  $H + e^{\eta(t)} \sum_a \lambda^a \psi_a(q)$ , where  $H$  is the Hamiltonian (13). In particular, the method (20) can be constrained to yield [10]

$$\begin{aligned}
p_{k+1/2} &= e^{-\Delta\eta_k} \Lambda_g(q_k) [p_k - (\delta t/2) \partial_q V(q_k)], \\
\bar{p}_{k+1/2} &= p_{k+1/2} - (\delta t/2) e^{-\Delta\eta_k} [\partial_q \psi(q_k)]^\top \lambda, \\
q_{k+1} &= q_k - \delta t \cosh(\Delta\eta_k) g^{-1} \bar{p}_{k+1/2}, \\
0 &= \psi_a(q_{k+1}) \quad (a = 1, \dots, m), \\
p_{k+1} &= \Lambda_g(q_{k+1}) [e^{-\Delta\eta_k} \bar{p}_{k+1/2} - (\delta t/2) \partial_q V(q_{k+1})],
\end{aligned} \tag{24}$$

where we have the projector  $\Lambda_g(q) \equiv I - R_g^{-1}(q) \partial_q \psi(q) g^{-1}$  with  $R_g(q) \equiv \partial_q \psi(q) g^{-1} \partial_q \psi(q)^\top$ , and  $(\partial_q \psi)_{ij} \equiv \partial \psi_i / \partial q^j$  is the Jacobian matrix of the constraints;  $\lambda = (\lambda_1, \dots, \lambda_m)^\top$  is the vector of Lagrange multipliers and  $\Delta\eta_k \equiv \int_{t_k}^{t_{k+1/2}} \gamma(t) dt$  accounts for the damping. In practice, the Lagrange multipliers are determined by solving the (nonlinear) algebraic equations for the constraints, i.e., the 2nd to 4th updates above are solved simultaneously. The above method consists in a dissipative generalisation of the well-known RATTLE integrator from molecular dynamics [100–103].

It is possible to generalise any other (conservative) symplectic method to this (dissipative) optimisation setting on manifolds. In this general setting, there still exists a shadow Hamiltonian so that convergence rates and stability are closely preserved numerically [10] (similarly to (18) and (19)). In particular, one can also consider different types of kinetic energy, beyond the quadratic case discussed above, which may perform better in specific problems [8]. This approach therefore allows one to adapt existing symplectic integrators to solve optimisation problems on Lie groups and other manifolds commonly appearing in machine learning, such as Stiefel, Grassmannians, or to solve constrained optimisation problems on  $\mathbb{R}^n$ .

## 2.5 Gradient flow as a high friction limit

Let us provide some intuition why simulating 2nd order systems is expected to yield faster algorithms. It has been shown that several other accelerated optimisation methods<sup>8</sup> are also discretisations of system (8) [38]. Moreover, in the large friction limit,  $\gamma \rightarrow \infty$ , this system reduces to the 1st order gradient flow,  $dq/dt = -\partial_q V(q)$  (assuming  $g \propto I$ ), which is the continuum limit of standard, i.e., nonaccelerated methods [38]. The same happens in more general settings; when the damping is too strong, the second derivative becomes negligible and the dynamics is approximately 1st order.

As an illustration, consider Figure 1 (left) where a particle immersed in a fluid falls under the influence of a potential force  $-\partial_q V(q)$ , that plays the role of “gravity”, and is constrained to move on a surface. In the *underdamped* case, the particle is under water, which is not so viscous, so it has acceleration and moves fast (even oscillate). In the *overdamped* case, the particle is in a highly viscous fluid, such as honey, and the drag force  $-\gamma p$  is comparable or stronger to  $-\partial_q V(q)$ , thus the particle moves slowly since it cannot accelerate; during the same elapsed time  $\delta t$ , an accelerated particle would travel a longer distance. We can indeed verify this behaviour numerically. In Figure 1 (right) we run algorithm (23) in the underdamped and overdamped regimes when solving

<sup>8</sup>Besides accelerated gradient based methods, accelerated extensions of important proximal-based methods such as proximal point, proximal-gradient, alternating direction method of multipliers (ADMM), Douglas-Rachford, Tseng splitting, etc., are implicit discretizations of (8); see [38] for details.

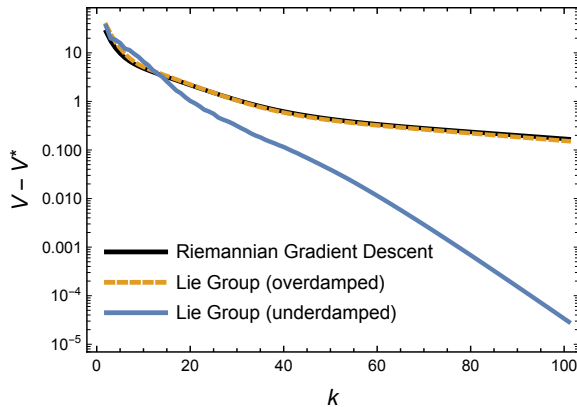
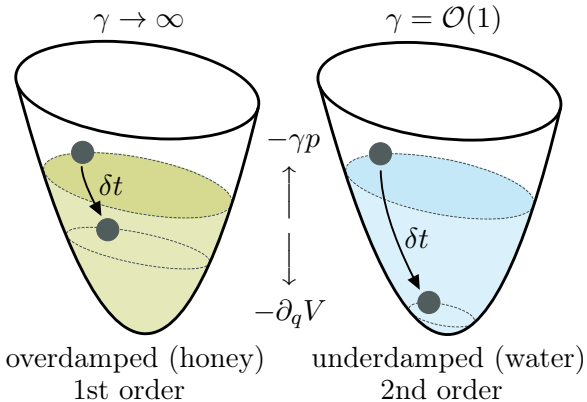


Figure 1: *Why simulating 2nd order systems yields accelerated methods.* *Left:* Constrained particle falling in fluids of different viscosity. When the drag force is strong the particle cannot accelerate and has a 1st order dynamics (see text). *Right:* Simulation of algorithm (23) where  $V(Q)$  is the energy of a spherical spin glass (Lie group  $SO(n)$ , with  $n = 500$ ) [10]. In the overdamped regime the method is close to Riemannian gradient descent [104], which is a 1st order dynamics; (23) is much faster in the underdamped regime.

an optimisation problem on the  $n$ -sphere, i.e., on the Lie group  $SO(n)$ .<sup>9</sup> We can see that, in the overdamped regime, this method has essentially the same dynamics as the Riemannian gradient descent [104], which is nonaccelerated and corresponds to a 1st order dynamics; all methods use the same step size, only the damping coefficient is changed.

## 2.6 Optimisation on the space of probability measures

There is a tight connection between sampling and optimisation on the space of probability measures which goes back to [50, 51]. Let  $\mathcal{P}_2(\mathbb{R}^n)$  be the space of probability measures on  $\mathbb{R}^n$  with finite second moments, endowed with a Wasserstein-2 metric  $W_2$ . The *gradient flow* of a functional  $F[\mu]$  on the space of probability measures is the solution to the partial differential equation  $\partial_t \mu(q, t) = -\nabla_{W_2} F[\mu(q, t)]$ , which, under sufficient regularity conditions, is equivalent to [50, 51, 105]

$$\partial_t \mu = \partial \cdot \left( \mu \partial \frac{\delta F[\mu]}{\delta \mu} \right), \quad (25)$$

where  $\partial \equiv \partial_q$  and  $\partial \cdot$  are the derivative and the divergence operators on  $\mathbb{R}^n$ , respectively. The evolution of this system solves the optimisation problem

$$\rho \equiv \arg \min_{\mu \in \mathcal{P}_2(\mathbb{R}^n)} F[\mu], \quad (26)$$

i.e.,  $\mu(q, t) \rightarrow \rho(q)$  as  $t \rightarrow \infty$  in the sense of distributions. We can consider the analogous situation with a dissipative flow induced by the conformal Hamiltonian tensor (7) on the space of probability measures; we set  $g = I$  and  $\gamma(t) = \gamma = \text{const.}$  for simplicity. Thus, instead of (25), we have a *conformal Hamiltonian system in Wasserstein space* given by the continuity equation

$$\partial_t \mu = \partial \cdot \left( \mu B \partial \frac{\delta F[\mu]}{\delta \mu} \right), \quad (27)$$

<sup>9</sup>The details are not important here, but this problem minimises the Hamiltonian of a spherical spin glass (see [10] for details). The same behaviour is seen with the constrained method (24) as well.

where now  $\partial \equiv (\partial_q, \partial_p)$  and  $\mu$  is a measure over  $\mathcal{P}_2(\mathbb{R}^{2d})$ . Let  $F$  be the *free energy* defined as

$$F[\mu] \equiv U[\mu] - \beta^{-1} S[\mu], \quad U[\mu] \equiv \mathbb{E}_\mu[H], \quad S[\mu] \equiv \mathbb{E}_\mu[-\log \mu], \quad (28)$$

where  $U$  is the (internal) energy,  $H$  is the Hamiltonian (6),  $S$  is the Shannon entropy, and  $\beta$  is the inverse temperature. The functional derivative of the free energy equals

$$\frac{\delta F}{\delta \mu} = H + \beta^{-1} \log \mu = \frac{1}{2} \|p\|^2 + V(q) + \beta^{-1} \log \mu. \quad (29)$$

In particular, the minimiser of  $F$  is the stationary density

$$\rho(q, p) = Z_\beta^{-1} e^{-\beta H(q, p)}, \quad Z_\beta \equiv \mathbb{E}_\mu[e^{-\beta H(q, p)}]. \quad (30)$$

Note also that the free energy (28) is nothing but the KL divergence (up to a constant which is the partition function):

$$\text{KL}[\mu \mid \rho] \equiv \mathbb{E}_\mu[\log(\mu/\rho)] = \beta F[\mu] - \log Z_\beta.$$

Therefore, the evolution of  $\mu$  as given by the conformal Hamiltonian system (27) minimises the divergence from the stationary density (30). Replacing (29) into (27) we obtain

$$\partial_t \mu = -\partial_q \cdot [\mu p] + \partial_p \cdot [\mu \partial_q V(q) + \gamma \mu p] + \gamma \beta^{-1} \partial_p^2 \mu,$$

which is nothing but the Fokker-Planck equation associated to the *underdamped* Langevin diffusion

$$dq_t = p_t dt, \quad dp_t = -\partial_q V(q_t) dt - \gamma p_t dt + \sqrt{2\gamma\beta^{-1}} dw_t, \quad (31)$$

where  $w_t$  is a standard Wiener process. Thus, the underdamped Langevin can be seen as performing *accelerated* optimisation on the space of probability measures. A quantitative study of its speed of convergence is given by the theory of hypocoercivity [106–108].

The above results provide a tight connection between sampling and optimisation. Interestingly, by the same argument as used in section 2.5 (see Figure 1), the high friction limit,  $\gamma \rightarrow \infty$ , of the underdamped Langevin diffusion (31) yields the *overdamped Langevin diffusion* [38, 107]

$$dq_t = -\nabla V(q_t) dt + \sqrt{2\beta^{-1}} dw_t, \quad (32)$$

which corresponds precisely to the gradient flow (25) on the free energy functional  $F[\mu]$  [51, 105], where now  $\mu = \mu(q, t) \in \mathcal{P}_2(\mathbb{R}^d)$ . Thus, in the same manner that a 2nd order damped Hamiltonian system may achieve accelerated optimisation compared to a 1st order gradient flow, the underdamped Langevin diffusion (31) may achieve accelerated sampling compared to the overdamped Langevin diffusion (32). Such an acceleration has indeed been demonstrated [109] in continuous-time and for a particular discretisation.

### 3 Hamiltonian-based accelerated sampling

The purpose of sampling methods is to efficiently draw samples from a given target distribution  $\rho$  or, more commonly, to calculate expectations with respect to  $\rho$ :

$$\int_{\mathcal{X}} f d\rho \approx \frac{1}{n} \sum_{k=0}^{n-1} f(x_k). \quad (33)$$

However, generating i.i.d. samples  $\{x_k\}$  is usually practically infeasible, even for finite sample spaces, as in high dimensions probability mass tends to concentrate in small regions of the sample space, while regions of high probability mass tend to be separated by large regions of negligible probability. Moreover,  $\rho$  is usually only known up to a normalisation constant [110]. To circumvent this issue, MCMC methods rely on constructing ergodic Markov chains  $\{x_n\}_{n \in \mathbb{N}}$  that preserve the target distribution  $\rho$ . If we run the chain long enough ( $n \rightarrow \infty$ ), Birkhoff’s ergodic theorem guarantees that the estimator on the right-hand side of (33) converges to our target integral on the left-hand side almost surely [111]. An efficient sampling scheme is one that minimises the variance of the MCMC estimator. In other words, fewer samples will be needed to obtain a good estimate. Intuitively, good samplers are Markov chains that converge as fast as possible to the target distribution.

### 3.1 Optimising diffusion processes for sampling

As many MCMC methods are based on discretising continuous-time stochastic processes, the analysis of continuous-time processes is informative of the properties of efficient samplers.

Diffusion processes possess a rich geometric theory, extending that of vector fields, and have been widely studied in the context of sampling. They are Markov processes featuring almost surely continuous sample paths (i.e., no jumps) and correspond to the solutions of stochastic differential equations (SDEs). While a deterministic flow is given by a first order differential operator—namely, a vector field  $X$  as used in §2—diffusions require specifying a set of vector fields  $X, Y_1, \dots, Y_N$ , where  $X$  represents the (deterministic) drift and  $Y_i$  the directions of the (random) Wiener processes  $w_t^i$ , and are characterised by a second order differential operator of the form  $\mathcal{L} \equiv X + Y_i \circ Y_i$ , known as the generator of the process. Equivalently, diffusions can be written as Stratonovich SDEs:  $dx_t = X(x_t)dt + Y_i(x_t) \circ dw_t^i$ .

For a smooth positive target measure  $\rho$ , the *complete* family of  $\rho$ -preserving diffusions is given by (up to a topological obstruction contribution) [112]

$$dx_t = \text{curl}_\rho(A)dt + \frac{1}{2}\text{div}_\rho(Y_i)Y_i dt + Y_i \circ dw_t^i, \quad (34)$$

for a choice of antisymmetric bracket  $A$ . Here  $\text{curl}_\rho$  is a differential operator on multi-vector fields, generalising the divergence on vector fields  $\text{div}_\rho$  of  $\rho$ , and is induced via an isomorphism  $\rho^\sharp$  defined by  $\rho$  which allows to transfer the calculus of twisted differential forms to a *measure-informed* calculus on multi-vector fields [112]. The ergodicity of (34) is essentially characterised by Hörmander’s *hypoellipticity* condition; i.e., whether the Lie algebra of vector fields generated by  $\{Y_i, [X, Y_i]\}_{i=1}^N$  spans the tangent spaces at every point [107, 113, 114]. On Euclidean space the above complete class of measure preserving diffusions can be given succinctly by Itô SDEs [115]:

$$dx_t = -(A + S)(x_t) \partial V(x_t) dt + \partial \cdot (A + S)(x_t) dt + \sqrt{2S(x_t)} dw_t, \quad (35)$$

where  $S, A$  reduce to symmetric and antisymmetric matrix fields and  $V$  is the negative Lebesgue log-density of  $\rho$ .

There are two well-studied criteria describing sampling efficiency in Markov processes: 1) the worst-case asymptotic variance of the MCMC estimator (33) over functions in  $L^2(\rho)$ , and 2) the spectral gap. The spectral gap is the lowest non-zero eigenvalue of the (negative) generator  $-\mathcal{L}$  on  $L^2(\rho)$ . When it exists, it is an exponential convergence rate of the density of the process to the target density [107, 116, 117]. Together, these criteria yield confidence intervals on the non-asymptotic variance of the MCMC estimator, which determines sampling performance [118].

A fundamental criterion for efficient sampling is non-reversibility [116, 119, 120]. A process is non-reversible if it is statistically distinguishable from its time-reversal when initialised at the target distribution [107]. Measure-preserving diffusions are non-reversible precisely when  $A \neq 0$  [121]. Intuitively, non-reversible processes backtrack less often and thus furnish more diverse samples [122]. Furthermore, non-reversibility leads to mixing, which accelerates convergence to the target measure. It is well known that removing non-reversibility worsens the spectral gap and the asymptotic variance of the MCMC estimator [116, 119, 120]. In diffusions with linear coefficients, one can construct the optimal non-reversible matrix  $A$  to optimise the spectral gap [123, 124] or the asymptotic variance [120]. However, there are no generic guidelines on how to optimise non-reversibility in arbitrary diffusions. This suggests a two-step strategy to construct efficient samplers: 1) optimise reversible diffusions, and 2) add a non-reversible perturbation  $A \neq 0$  [125].

Diffusions on manifolds are reversible when  $A \equiv 0$ , and thus have the form  $dx_t = \frac{1}{2} \operatorname{div}_\rho(Y_i) Y_i dt + Y_i \circ dw_t^i$ , which on Euclidean space reads

$$dx_t = -S(x_t) \partial V(x_t) dt + \partial \cdot S(x_t) dt + \sqrt{2S(x_t)} dw_t. \quad (36)$$

The spectral gap and the asymptotic variance of the MCMC estimator are the same optimality criteria in reversible Markov processes [126]. When  $S$  is positive definite everywhere, it defines a Riemannian metric  $g$  on the state space. The generator is then the elliptic differential operator

$$\mathcal{L} = \nabla_g + \Delta_g, \quad (37)$$

where  $\nabla_g$  is the Riemannian gradient and  $\Delta_g$  is the Laplace-Beltrami operator, i.e., the Riemannian counterpart of the Laplace operator. Thus, reversible (elliptic) diffusions (37) are the natural generalisation of the overdamped Langevin dynamics (32) to Riemannian manifolds [127]. Optimising  $S$  to improve sampling amounts to endowing the state space with a suitable Riemannian geometry that exploits the structure of the target density. For example, sampling is improved by directing noise along vector fields that preserve the target density [128]. When the potential  $V$  is strongly convex, the optimal Riemannian geometry is given by  $g \equiv \partial^2 V$  [129, 130]. Sampling can also be improved in hypoelliptic diffusions with degenerate noise (i.e., when  $S$  is not positive definite). Intuitively, the absence of noise in some directions of space leads the process to backtrack less often and thus yield more diverse samples. For instance, in the linear case, the optimal spectral gap is attained for an irreversible diffusion with degenerate noise [131]. However, degenerate diffusions can be very slow to start with, as the absence of noise in some directions of space make it more difficult for the process to explore the state space [131].

Underdamped Langevin dynamics (31) combines all the desirable properties of an efficient sampler: it is irreversible, has degenerate noise, and achieves accelerated convergence to the target density [132]. We can optimise the reversible part of the dynamics (i.e., the friction  $\gamma$ ) to improve the asymptotic variance of the MCMC estimator [133]. Lastly, we can significantly improve underdamped Langevin dynamics by adding additional non-reversible perturbations to the drift [134].

One way to obtain MCMC algorithms is to numerically integrate diffusion processes. As virtually all non-linear diffusion processes cannot be simulated exactly, we ultimately need to study the performance of discrete algorithms instead of their continuous counterparts. Alarming, many properties of diffusions can be lost in numerical integration. For example, numerical integration can affect ergodicity [135]. An irreversible diffusion may sample more poorly than its reversible counterpart after integration [136]. This may be because numerical discretisation can introduce, or otherwise change, the amount of non-reversibility [136]. The invariant measure of the diffusion and its numerical integration may differ, a feature known as bias. We may observe very large bias even in the simplest schemes, such as the Euler-Maruyama integration of overdamped Langevin [60].

Luckily, there are schemes whose bias can be controlled by the integration step size [137]; yet, this precludes using large step sizes. Alternatively, one can remove bias by supplementing the integration step with a Metropolis-Hastings corrective step; however, this makes the resulting algorithm reversible. In conclusion, designing efficient sampling algorithms with strong theoretical guarantees is a non-trivial problem that needs to be addressed in its own right.

### 3.2 Hamiltonian Monte Carlo

Constructing measure-preserving processes, in particular diffusions, is relatively straightforward. A much more challenging task consists of constructing efficient *sampling algorithms* with strong theoretical guarantees. We now discuss an important family of well-studied methods, known as *Hamiltonian Monte Carlo* (HMC), which can be implemented on any manifold, for any smooth fully supported target measure that is known up to a normalising constant. Some of these methods can be seen as an appropriate geometric integration of the underdamped Langevin diffusion, but it is in general simpler to view them as combining a geometrically integrated deterministic dynamics with a simple stochastic process that ensures ergodicity.

The *conservative* Hamiltonian systems previously discussed provide a natural candidate for the deterministic dynamics. Indeed, given a target measure  $\rho \propto e^{-V} \mu_{\mathcal{M}}$ , with  $\mu_{\mathcal{M}}$  a Riemannian measure (such as the Lebesgue measure  $dq$  on  $\mathcal{M} = \mathbb{R}^d$ ), if we interpret the negative log-density  $V(q)$  as a potential energy, i.e., a function depending on *position*  $q$ , one can then plug in the potential within Newton's equation to obtain a deterministic proposal that is well-defined on any manifold, as soon as the acceleration and derivative operators have been replaced by their curved analogues

$$\underbrace{m\ddot{q} = -\partial V(q)}_{\text{flat Newton}} \longrightarrow \underbrace{\frac{\overbrace{\frac{\nabla \dot{q}}{dt}}^{\text{acceleration}}}{\text{Riemannian Newton}} = \overbrace{-\nabla V(q)}^{\text{direction of greatest decrease}}}_{\text{Riemannian Newton}}, \quad (38)$$

with given initial conditions for the position  $q$  and *velocity*  $v = dq/dt$ . This is a 2nd order system which evolves in the tangent bundle,  $(q, v) \in T\mathcal{M}$ , which is  $T\mathcal{M} = \mathbb{R}^d \times \mathbb{R}^d$  when  $\mathcal{M} = \mathbb{R}^d$ . The resulting flow is conservative since it corresponds to a Hamiltonian system as discussed in section §2.2, with Hamiltonian  $H(q, v) \equiv \frac{1}{2}\|v\|_q^2 + V(q)$ , where  $\|v\|_q^2$  is the Riemannian squared-norm, which is  $v^T g(q)v$  when  $\mathcal{M} = \mathbb{R}^d$  and  $g(q)$  is the Riemannian metric; this is the manifold version of the Hamiltonian (6). This system preserves the symplectic measure  $\mu_{\Omega}(q, v) = \det g(q) dq dv$ , and thus also the *canonical distribution*  $\mu \propto e^{-H(q,v)} \mu_{\Omega}$ , which is the product of the target distribution over position with the Gaussian measures on velocity (with covariance  $g$ ). For instance, on  $\mathcal{M} = \mathbb{R}^d$ ,

$$\mu(q, v) \propto \rho(q) \times \mathcal{N}(0, g^{-1}(q))(v) \propto e^{-V(q)} \sqrt{\det g(q)} dq \times \sqrt{\det g(q)} e^{-\frac{1}{2}v^T g(q)v} dv.$$

Moreover, the pushforward under the projection  $\text{Proj} : (q, v) \mapsto q$  is precisely the target measure:  $\text{Proj}_* \mu = \rho$ . Concretely, the samples generated by moving according to Newton's law, after ignoring their velocity component, have  $\rho$  as their law. The main critical features and advantages in using Hamiltonian systems arises from their numerical implementation. Indeed, the flow of (38) is only tractable for the simplest target measures, namely those possessing a high degree of symmetry. In order to proceed, we must devise suitable numerical approximations which, unfortunately, not only break such symmetries but may lose key properties of the dynamics such as stationarity (typically not retained by discretisations). However, as we saw in section §2.2, most *symplectic integrators* have a *shadow Hamiltonian* and thus generate discrete trajectories that are close to the associated bona fide (shadow) Hamiltonian dynamics, that in particular preserve the shadow canonical distribution.



Most integrators used in sampling, such as the leapfrog, are *geodesic integrators*. These are *splitting methods* (see section §2.1) obtained by splitting the Hamiltonian  $H(q, v) = H_1(q, v) + H_2(q)$ , where  $H_1(q, v) = \frac{1}{2}\|v\|_q^2$  and  $H_2(q) = V(q)$  are to be treated as independent Hamiltonians in their own right. Both of these Hamiltonians generate dynamics that might be tractable: the Riemannian component  $H_1$ , associated to the Riemannian reference measure, induces the geodesic flow, while the target density component  $H_2$  gives rise to a vertical gradient flow, wherein the velocity is shifted by the direction of maximal density change, i.e.,  $(q, v) \mapsto (q, v - \delta t \nabla_q V(q))$ . The Jacobi identity and the BCH formula imply these integrators do possess a shadow Hamiltonian  $\tilde{H}$ , and reproduce its dynamics. Such a shadow can in fact be explicitly obtained from (5) by computing iterated Poisson brackets; e.g., on  $\mathcal{M} = \mathbb{R}^d$  and for  $H(q, v) = (1/2)v^T g v + V(q)$ , the three-stage geodesic integrator  $\Phi_{b\delta t}^{H_1} \circ \Phi_{a\delta t}^{H_2} \circ \Phi_{(1-\frac{1}{2}b)\delta t}^{H_1} \circ \Phi_{(1-2a)\delta t}^{H_2} \circ \Phi_{(1-\frac{1}{2}b)\delta t}^{H_1} \circ \Phi_{a\delta t}^{H_2} \circ \Phi_{b\delta t}^{H_1}$ , with parameters  $a, b \in \mathbb{R}$ , yields [138]

$$\tilde{H}(q, v) = H(q, v) + \delta t^2 [c_1 \partial V(q)^T g^{-1} \partial V(q) + c_2 v^T \partial^2 V(q) v] + O(\delta t^4),$$

for some constants  $c_1$  and  $c_2$ . As an immediate consequence, these symplectic integrators preserve the reference symplectic measure  $\mu_\Omega$  and can be used as a (deterministic) Markov proposal, which when combined with the Metropolis-Hastings acceptance step that depends only on the target density, gives rise to a measure-preserving process. Moreover, the existence of the shadow Hamiltonian ensures that the acceptance rate will remain high for distant proposals, allowing small correlations. However, since Hamiltonian flows are conservative, they remain stuck within energy level sets, which prevents ergodicity. It is thus necessary to introduce another measure-preserving process, known as the heat bath or thermostat, that explores different energy levels; the simplest such process corresponds to sampling a velocity from a Gaussian distribution. Bringing these ingredients together, we thus have the following HMC algorithm: given  $z^n = (q, v)$ , compute  $z^{n+1}$  according to

1. *Heat bath*: sample a velocity according to a Gaussian,  $v^\dagger \sim \mathcal{N}(0, g^{-1}(q))$ .
2. *Shadow Hamiltonian dynamics*: move along the Hamiltonian flow generated by the geodesic integrator,  $z^* = \Psi_{\delta t}(z^\dagger)$ , where  $z^\dagger = (q, v^\dagger)$ .
3. *Metropolis correction*: accept  $z^*$  with probability  $\min\{1, e^{-\Delta H}\}$ , where  $\Delta H = H(z^*) - H(z^\dagger)$ . If accepted then set  $z^{n+1} = z^*$ , otherwise set  $z^{n+1} = (q, -v^\dagger)$ .

The above rudimentary HMC method (originally known as Hybrid Monte Carlo) was proposed for simulations in lattice quantum chromodynamics with  $\mathcal{M}$  being the special unitary group,  $SU(n)$ , and used a Hamiltonian dynamics ingeniously constructed from the Maurer-Cartan frame to compute the partition function of discretised gauge theories [13]. This method has later been applied in molecular dynamics and statistics [12, 49, 64, 139, 140].

While the above discussion provides a justification for the use of Hamiltonian mechanics, a more constructive argument from first principles can also be given. From the family of measure-preserving dynamics, which as we have seen can be written as  $\text{curl}_\mu(A)$  (recall (34)), we want to identify those suited to practical implementations (here  $\mu$  could be any distribution on some space  $\mathcal{F}$  having the target  $\rho$  has a marginal). Only for the simplest distributions  $\mu$  we can hope to find brackets  $A$  for which the flow of  $\text{curl}_\mu(A)$  is tractable. Instead, the standard approach to geometrically integrate this flow relies as before on splitting methods, which effectively decompose  $\mu \propto e^{-\sum H_\ell} \mu_{\mathcal{F}}$  into simpler components by decomposing the reference measure from the density and taking advantage of any product structure of the density, so that  $\text{curl}_\mu(A) = \text{curl}_{\mu_{\mathcal{F}}}(A) + \sum_\ell X_{H_\ell}^A$ .

There are three critical properties underpinning the success of HMC in practice. The first two are the preservation of the reference measure and the existence of a conserved shadow Hamiltonian

for the numerical method. These imply that we remain close to preserving  $\mu$  along the flow, and in particular leads to Jacobian-free Metropolis corrections with good acceptance rates for distant proposals (see [141] for examples of schemes with Jacobian corrections). Achieving these properties yield strong constraints on the choice of  $A$  [142]; the shadow property is essentially exclusive to Poisson systems, for which the conservation of a common reference measure is equivalent to the triviality of the modular class in the first Poisson cohomology group [143]. In particular, Poisson brackets that admit such an *invariant measure* have been carefully analysed and are known as *unimodular*; the only unimodular Poisson bracket that can be constructed on general manifolds seems to be precisely the symplectic one.

The third critical property is the existence of splittings methods for which all the composing flows are either tractable or have adequate approximations, namely the geodesic integrators. Indeed, as we have seen, the flow  $\Phi^{H_2}$ —induced by the potential  $H_2(q) = V(q)$ —is always tractable, independently of the complexity of the target density; this is possible mainly due to the extra “symmetries” resulting from implementing the flow on a higher-dimensional space  $T\mathcal{M}$  rather than  $\mathcal{M}$ . On the other hand, one key consideration for the tractability of the the geodesic flow  $\Phi_{\delta t}^{H_1}$ —induced by the kinetic energy  $H_1(q, v)$ —is the choice of Riemannian metric; for most cases, it is numerically hard to implement  $\Phi_{\delta t}^{H_1}$  since several implicit equations need to be solved. In general, it is desirable to use a Riemannian metric that reflects the intrinsic symmetries of the sample space, mathematically described by a Lie group action. Indeed, by using an *invariant* Riemannian metric, one greatly simplifies the equations of motion of the geodesic flow, reducing the usual 2nd order Euler-Langrange equations to the 1st order Euler-Arnold equations [144–146], with tractable solutions in many cases of interest, e.g., for naturally reductive homogeneous spaces; including  $\mathbb{R}^d$ , the space of positive definite matrices, Stiefel manifolds, Grassmannian manifolds, and many Lie groups. In such cases, it is possible to find a Riemannian metric whose geodesic flow is known and given by the Lie group exponential [16, 147, 148]. For the other main class of spaces, namely those given by constraints, if one chooses the restriction of the Euclidean metric, then the RATTLE scheme discussed in optimisation (see section §2.4) is a suitable symplectic integrator [103, 149–152] (perhaps up to a reversibility check). Occasionally, it may be suitable to use a Riemannian metric associated to the target distribution rather than the sample space; e.g., when it belongs to a statistical manifold. In that case, any choice of (information) divergence gives rise to an information tensor that may be used in the HMC algorithm. Notably, this is the case in Bayesian statistics, wherein attempting to find a Riemannian metric that locally matches the Hessian of the posterior motivates the use of the Fisher information tensor summed with the Hessian of the prior, giving rise to the Riemannian HMC [127, 153]. When a Riemannian metric whose geodesic flow is unknown is chosen, one can use the trick of increasing the dimension of the phase space to add symmetries to derive explicit symplectic integrators [154, 155].

Once we have an integrator for the geodesic flow, another important consideration is the construction and tuning of the overall integrator, i.e., the specific composition of  $\Phi_{\delta t}^{H_1}$  and  $\Phi_{\delta t}^{H_2}$ . Traditional numerical integrators are tuned to provide highly accurate approximations for the trajectories in the limit  $\delta t \rightarrow 0$ ; for instance, a forth order Runge-Kutta method. However, samplers aim to have the largest possible step size  $\delta t$  in order to reduce correlations. One approach consists in tuning the integrator to obtain good density preservation in the Gaussian case. Another approach consists in tuning the integrator to ensure the shadow Hamiltonian  $\tilde{H}$  agrees with  $H$  up to the desired order; see [156–161]. We note that when the target density contains two components, one computationally expensive and the other computationally cheap, it may be desirable to further split the potential  $H_2(q) = V(q)$  to obtain higher acceptance rates [162–164]. In order to achieve ergodicity in HMC methods, it is usually sufficient to randomise the trajectory length of the integrator [165–167]. However, deriving guarantees on the rate of convergence of HMC is difficult, though recent work have

established sufficient conditions for geometric ergodicity [15, 168].

Let us also briefly mention some useful upgrades that have been proposed in recent years. First, whenever the Metropolis step rejects the proposed sample, the (expensive) computation of the numerical trajectory is wasted, and several modifications have been proposed to address this issue, for example by granting the method extra integration steps when the proposal is rejected [169, 170], or using a dynamic integration with a termination criterion that aims to ensure the motion is long enough to avoid random walks, but short enough that we do not waste computational effort, such as the No-U-Turn sampler [171].

Second, the Metropolis algorithm gives rise to a *reversible* method which, as discussed above, usually has slower convergence properties. Modern HMC methods bypass this issue by replacing the heat bath by an Ornstein-Uhlenbeck process, which ensures the overall algorithm is *irreversible*. In this case, the overall HMC method can be viewed as a geometric integration of the underdamped Langevin diffusion [106, 172, 173]. The connection between HMC and Langevin diffusion originates from the desire to replace the Gaussian heat bath with a partial momentum refreshment, yielding a more accurate simulation of dynamical properties and higher acceptance rates [174].

Third, many modifications of the rudimentary HMC algorithm only provide improvements when the acceptance rate is sufficiently high. A third class of upgrades improves the acceptance rate by using the fact that the shadow Hamiltonian is exactly preserved by the integrator. These *shadow HMC* methods sample from a biased target distribution, defined by the (truncated) shadow Hamiltonian, and correct the bias in the samples via an importance sampler [138, 175, 176].

Finally, the Metropolis step can be replaced with a multinomial correction that uses the entire numerical trajectory, accepting a given point along it according to the degree by which it distorts the target measure [64]. Some methods entirely skip the accept/reject step, in particular those relying on approximate gradients and surrogates [177, 178], such as the *stochastic* HMC methods; such methods approximate the potential  $V(q)$  and its derivative when they are given by a sum over data points,  $V(q) = \sum_i V_i(q)$ , by a cheaper sum over a uniformly sampled minibatches [179] (these are commonly called stochastic gradients in machine learning). However, this may break the shadow property and reduce the scalable and robust properties of HMC methods [180].

## 4 Statistical inference with kernel-based discrepancies

The problem of *parameter inference* consists of estimating an element  $\theta^* \in \Theta$  using a sequence of random functions (or estimators)  $\hat{\theta}_n : \Omega \rightarrow \Theta$ , with  $\hat{\theta}_n$  determined by a set of measurements  $\{q_1, \dots, q_n\}$  representing the available experimental data. In the statistical context, we search for the optimal approximation  $\mu_{\theta^*}$  of the target measure  $\rho$  within a statistical model  $\{\mu_\theta : \theta \in \Theta\}$ , with respect to a *discrepancy*  $D : \mathcal{P} \times \mathcal{P} \rightarrow [0, \infty]$  over the set of probability measures  $\mathcal{P}$ . A common choice of discrepancy is the KL-divergence, and the resulting inference problem can be implemented via the asymptotically optimal maximum likelihood estimators [69]. As in many applications we are interested in computing expectations, a particularly suitable notion of discrepancies are the *integral probability pseudometrics* (IPM) [181], which quantify the worse-case integration error with respect to a family of functions  $\mathcal{F}$

$$d_{\mathcal{F}}(\rho, \mu) \equiv \sup_{f \in \mathcal{F}} \left| \int f d\rho - \int f d\mu \right|.$$

An apparent difficulty arises with IPMs in that we need to compute a supremum, which will be intractable for most choices of  $\mathcal{F}$ . Observe, however, that if  $\mathcal{F}$  were the unit ball of a normed vector space  $\mathcal{H}$ , and integration with respect to  $\rho$  and  $\mu$  was a continuous linear functional on  $\mathcal{H}$ , then  $d_{\mathcal{F}}(\rho, \mu)$  would correspond to the distance between  $\rho$  and  $\mu$  in the dual norm over the dual  $\mathcal{H}^*$ ,

i.e.,  $d_{\mathcal{F}}(\rho, \mu) = \|\rho - \mu\|_*$ . Conveniently, reproducing kernel Hilbert spaces (RKHS) are precisely Hilbert spaces over which the Dirac distributions  $\delta_x : f \mapsto f(x)$  act continuously [182–184], and, more generally, the probability distributions that act continuously by integration on a RKHS  $\mathcal{H}$  are exactly those for which all elements of  $\mathcal{H}$  are integrable [185]. Denoting by  $\mathcal{P}_{\mathcal{H}}$  the set of such probability measures, so that by definition  $\delta_x \in \mathcal{P}_{\mathcal{H}}$ , we can define the *Maximum Mean Discrepancy* (MMD) as

$$\text{MMD} : \mathcal{P}_{\mathcal{H}} \times \mathcal{P}_{\mathcal{H}} \rightarrow [0, \infty), \quad \text{MMD}[\rho \mid \mu] = \|\rho - \mu\|,$$

where we further used the Riesz representation isomorphism to view  $\rho, \mu \in \mathcal{P}_{\mathcal{H}} \subset \mathcal{H}^* \cong \mathcal{H}$  as elements of  $\mathcal{H}$ . The map  $\mathcal{P}_{\mathcal{H}} \rightarrow \mathcal{H}$  is usually referred to as the *mean embedding* [186, 187]. The angles between the mean embedding of Dirac distributions play a central role in the study of RKHS, and indeed characterise them. They define the *reproducing kernel*

$$k : \mathcal{M} \times \mathcal{M} \rightarrow \mathbb{R}, \quad k(x, y) \equiv \langle \delta_x, \delta_y \rangle,$$

with  $\langle \cdot, \cdot \rangle$  denoting the inner product on  $\mathcal{H}$ , from which we can obtain a practical expression for the squared MMD:

$$\text{MMD}^2[\rho \mid \mu] = \iint k(x, y)(\rho - \mu)(dy)(\rho - \mu)(dx).$$

#### 4.1 Topological methods for MMDs

A key feature of RKHS, as identified by Laurent Schwartz, is the fact they are *Hilbertian subspaces*, i.e., Hilbert spaces continuously embedded within a topological vector space  $\mathcal{T}$ , denoted  $\mathcal{H} \hookrightarrow \mathcal{T}$  [188]. In this context, by composing the transpose of the inclusion  $\mathcal{H} \hookrightarrow \mathcal{T}$  with the Riesz isomorphism, we can define a (generalised) mean embedding as the weakly-continuous positive map

$$\phi : \mathcal{T}^* \hookrightarrow \mathcal{H}^* \rightarrow \mathcal{H}.$$

This mapping allows us to transfer structures between  $\mathcal{H}$  and  $\mathcal{T}^*$ , an example of which is the MMD, which is nothing else than the pullback of the Hilbert space metric from  $\mathcal{H}$  to  $\mathcal{T}^*$ . Some important examples of  $\mathcal{T}$  are  $C_0$ ,  $C_c^\infty$  and  $\mathbb{R}^{\mathcal{M}}$  (with their canonical topologies), whose duals are the spaces of finite Radon measures, Schwartz distributions, and measures with finite support, respectively [189]. In particular a RKHS, as defined above, is any Hilbert space satisfying  $\mathcal{H} \hookrightarrow \mathbb{R}^{\mathcal{M}}$ . More generally, when  $\mathcal{T}$  is continuously embedded in the space of  $\mathbb{R}^n$ -valued functions on  $\mathcal{M}$ —as in the examples above, which have  $n = 1$ —then  $\mathcal{H}$  inherits (and can be characterised in terms of) a reproducing kernel  $K : \mathcal{M} \times \mathcal{M} \rightarrow \mathbb{R}^{n \times n}$ , defined  $\forall v, u \in \mathbb{R}^n$  by

$$v^\top K(x, y)u = \delta_x^v [\phi(\delta_y^u)],$$

where  $\delta_x^u : h \mapsto u \cdot h(x)$ ; but this need not be the case in general, and we will employ Hilbertian subspaces with no reproducing kernel to construct the score-matching discrepancy.

This geometric description of RKHS and MMD allows us to swiftly apply topological methods in their analysis. For example, in order for  $\text{MMD}^2$  to be a valid notion of statistical divergence, it should accurately discriminate distinct distributions, in the sense that  $\text{MMD}[\rho \mid \mu] = 0$  iff  $\rho = \mu$ . By construction, MMD will be *characteristic to a subset of  $\mathcal{T}^*$* , that is be able to distinguish its elements, iff  $\phi$  is injective. The Hahn–Banach theorem further shows that this is equivalent to the denseness of  $\mathcal{H}$  in  $\mathcal{T}$ , reducing the matter to a topological question [186, 189, 190]. In many applications, we typically would like  $\mathcal{T}^*$  to be the set of probability measures, but the latter is not even a vector space. Instead, just as is commonly done to define (statistical) manifolds, it is

desirable to embed  $\mathcal{P}$  within a more structured space, such as the space of finite Radon measures  $C_0^*$ . Characteristicness to  $C_0^*$  is also known as *universality* in learning theory, since such RKHS are dense in  $L^2(\mu)$  for any  $\mu \in \mathcal{P}$ , which enables the method to learn the target function independently of the data-generating distribution [191]. However, in many important cases, we are interested in analysing the denseness of  $\mathcal{H}$  in a space other than  $C_0$ . For instance, in the case of unbounded reproducing kernels, we cannot aim to separate all finite distributions, since the RKHS will contain unbounded functions and the MMD will only be defined on a subset of  $\mathcal{P}$ . In the particular case of the KSDs discussed below, which are given by transforming a base RKHS into a Stein RKHS via a differential operator, the characteristicness of the Stein RKHS to a set of probability measures is equivalent to the characteristicness of the base RKHS to more general spaces  $\mathcal{T}^*$  of Schwartz distributions [185].

Moreover, the ability of MMD to discriminate distributions is also useful to ensure it further metrises, or at least controls, weak convergence, and thus provide a suitable quantification of the discrepancy between unequal distributions. Indeed, on non-compact locally compact Hausdorff spaces such as  $\mathbb{R}^d$ , when  $\mathcal{H} \hookrightarrow C_0$ , then MMD will metrise weak convergence (of probability measures) iff the kernel  $k$  is continuous and  $\mathcal{H}$  is characteristic to the space of finite Radon measures [192]. The fact that the RKHS must separate all finite measures in order to metrise weak convergence results from the fact that otherwise MMD cannot in general prevent positive measures from degenerating into the null measure on non-compact spaces, beyond the family of translation-invariant kernels, for which characteristicness to the sets of probability measures or that of finite measures are in fact equivalent [189]. It is also possible to prevent probability mass from escaping to infinity—when the topology of the sequence of distributions is relatively compact with respect to the weak topology on the space of distributions—since, in that case, standard topological arguments relate MMD and weak convergence via characteristicness to  $\mathcal{P}$  [193]. For example, by Prokhorov’s theorem we may use the tightness of a sequence of distributions to ensure characteristic MMDs detect any loss of mass, and thus control weak convergence [194].

## 4.2 Smooth measures and KSDs

MMD have a computationally tractable expression whenever  $\rho, \mu$  are discrete measures, or at least tractable  $U$ -statistics when their samples are readily available. Many applications involve distributions that are smooth and fully supported, but hard to sample from. Recalling the definition of  $d_{\mathcal{F}}(\rho, \mu)$ , it would be useful to construct a MMD for which the set  $\mathcal{F}$  consists of functions whose integral under  $\mu$  is tractable, for example equal to zero; the MMD would then reduce to a double integration with respect to  $\rho$ . To achieve this, we will leverage ideas from *Stein’s method* [195, 196], and apply Stein operators to a given RKHS so as to construct a *Stein RKHS* whose elements have vanishing expectation under a distribution of interest.

### 4.2.1 The canonical Stein operator and Poincaré duality

To gain intuition on Stein operators, we begin by considering the integral with respect to  $\mu$  as a linear operator on test functions,  $\mu : C_c^\infty(\mathcal{M}) \rightarrow \mathbb{R}$ , with  $\mu f \equiv \int f d\mu$ , and we are interested in generating test functions in the kernel of this operator (i.e., with vanishing expectations). There are two fundamental theorems that help us understand the integral-differential geometry of the manifold: de Rham’s theorem and Poincaré duality. The former relates the topology of the manifold to information on the solutions of differential equations defined over the manifold [197]. The latter (which contains the fundamental theorem of calculus) describes the properties of the integral pairing  $(\alpha, \beta) \mapsto \int \alpha \wedge \beta$  of differential forms, which include the pairing of test functions with smooth

measures  $(f, \mu) \mapsto \int f d\mu$ . While these results are canonical statements about the manifold, we can turn them into measure-theoretic statements by means of the isomorphism  $\mu^\sharp$ . In particular, when  $\mathcal{M}$  is connected, there is an isomorphism between the top compactly supported twisted de Rham cohomology group  $H_c^n(\mathcal{M})$  (which depends on the topology of  $\mathcal{M}$ ) and  $\mathbb{R}$  given by integration,  $\omega \mapsto \int_{\mathcal{M}} \omega$ . Applying the transformation  $\mu^\sharp$  to this isomorphism yields the isomorphism of vector spaces

$$\mu : C_c^\infty(\mathcal{M}) / \text{Im}(\text{div}_\mu|_c) \rightarrow \mathbb{R},$$

where  $\text{div}_\mu|_c : \mathfrak{X}_c(\mathcal{M}) \rightarrow C_c^\infty(\mathcal{M})$  is the divergence operator restricted to the set of compactly supported vector fields  $\mathfrak{X}_c(\mathcal{M})$ . Hence, if  $h, f \in C_c^\infty(\mathcal{M})$ , then

$$\int f d\mu = \int h d\mu \iff f = h + \text{div}_\mu(X) \quad \text{for some } X \in \mathfrak{X}_c(\mathcal{M}).$$

Consequently,

$$\mu^{-1}(\{0\}) = \{\text{div}_\mu(X) : X \in \mathfrak{X}_c(\mathcal{M})\}.$$

Thus, the test functions that integrate to zero are precisely those that can be written as the divergence of compactly supported vector fields. In particular, on compact manifolds, there is a canonical Stein operator,  $\text{div}_\mu$ , which turns vector fields into functions with vanishing expectations. For other types of manifolds, one can obtain similar *dualities* by using other classes of differential forms, such as the square-integrable ones, or by allowing boundaries. For our purposes, the above is sufficient to motivate calling

$$S_\mu \equiv \text{div}_\mu|_{\mathfrak{X}_\mu} : \mathfrak{X}_\mu \rightarrow C^\infty(\mathcal{M})$$

the *canonical Stein operator*, whose domain  $\mathfrak{X}_\mu$ , called the *Stein class*, is any set of vector fields satisfying the desired property that  $\mathbb{E}_\mu[S_\mu(X)] \equiv \int S_\mu(X) d\mu = 0$ , for all  $X \in \mathfrak{X}_\mu$ .

If we have a bracket  $B$  on  $\mathcal{M}$ , we can turn the canonical Stein operator on vector fields into a 2nd order differential operator acting on functions, the  $B$ -Stein operator on the Stein class

$$C_\mu^\infty \equiv \{f \in C^\infty(\mathcal{M}) : X_f^B \in \mathfrak{X}_\mu\},$$

by

$$S_\mu^B : C_\mu^\infty \rightarrow C^\infty(\mathcal{M}), \quad S_\mu^B f \equiv \text{div}_\mu(X_f^B).$$

If  $\mu = e^{-H} \mu_{\mathcal{M}}$  then we have the following useful decomposition:

$$\text{div}_{e^{-H} \mu_{\mathcal{M}}}(X_f^B) = \text{div}_{\mu_{\mathcal{M}}}(X_f^B) - X_f^B(H).$$

Let us give some important examples of bracket Stein operators. When  $B \equiv A$  is antisymmetric, the  $A$ -Stein operator is simply a 1st order differential operator, namely the  $\mu$ -preserving *curl vector field*  $S_\mu^A = \text{curl}_\mu(A)$ . When  $B$  is Riemannian, and  $\mu_{\mathcal{M}}$  is the Riemannian measure, then

$$S_\mu^g(f) = \nabla \cdot X_f^g - \langle \nabla f, \nabla H \rangle = \Delta f - \langle \nabla f, \nabla H \rangle = \Delta f + \langle \nabla f, \nabla \log d\mu/d\mu_{\mathcal{M}} \rangle,$$

where  $\nabla, \Delta, \nabla \cdot, \langle \cdot, \cdot \rangle$  are the Riemannian gradient, Laplacian, divergence, and metric, respectively; the  $g^{-1}$ -Stein operator becomes the Riemannian Stein operator [21, 198, 199]. Hence, the Riemannian Stein operator is the restriction of the canonical Stein operator to gradient vector fields. In general, decomposing the bracket into its symmetric and antisymmetric parts,  $B \equiv S + A$ , we obtain the following useful decomposition of the  $B$ -Stein operator:

$$S_\mu^{S+A}(f) = \text{div}_\mu(X_f^S) + \text{curl}_\mu(A)(f). \quad (39)$$

In particular, if we restrict ourselves to a symmetric positive semi-definite  $B$ , associated to a set of vector fields  $\{Y_i\}$ ,  $X_f^B \equiv Y_i(f)Y_i$  for any function  $f$ , then (39) corresponds to the generator of a  $\mu$ -preserving diffusion. A suitable Stein class is then the domain of the generator, since for any function in that domain  $\mathbb{E}_\mu [S_\mu^{S+A} f]$  vanishes by the Fokker-Planck equation. The construction of Stein operators via measure-preserving diffusions is known as the Barbour approach [200]. In fact, the brackets allow us to define a more general notion of Stein operator acting on 1-forms  $\{\alpha : X_\alpha^B \in \mathfrak{X}_\mu\}$ , and, on flat Euclidean space,  $S_\mu^B(\alpha) \equiv \text{div}_\mu(X_\alpha^B)$  recovers the ‘‘diffusion’’ Stein operator [201].

#### 4.2.2 Kernel Stein discrepancies and score matching

Once we have a Stein operator, we need to construct a Stein class for it, i.e., a set  $\mathcal{V}$  of vector fields (or more general tensor fields) whose image  $\mathcal{F}$  under the operator has mean zero under  $\mu$ . The resulting IPM is then known as a *Stein Discrepancy*:

$$d_{S_\mu(\mathcal{V})}(\mu, \rho) = \sup_{X \in \mathcal{V}} \left| \int S_\mu(X) d\rho \right|.$$

The expression  $\int S_\mu(X) d\rho$  is precisely the rate of change of the KL divergence along measures satisfying the continuity equation; an observation that leads to *Stein variational gradient descent* (SVGD) methods to approximate distributions [198, 202]. Specifically, in SVGD the target measure is approximated using a finite distribution  $\sum_\ell \delta_{x_\ell}$ , where the location of the *particles*  $\{x_\ell\}_\ell$  is updated by moving along the direction that maximises the rate of change of KL within a space of vector fields isomorphic to a RKHS (e.g., the space of gradients of functions in a RKHS).

When  $S_\mu$  is the canonical Stein operator, there is a canonical Stein class, provided by Stokes’ theorem, which essentially only depends on the manifold: for a connected manifold  $\mathcal{M}$ , viewing integration as an operator on smooth  $\mu$ -integrable functions, then  $\int f d\mu = 0 \iff \int d\alpha = 0$ , where  $f = \text{div}_\mu(\mu^\sharp(\alpha))$ . Unfortunately, Stokes’ theorem usually does not provide a practical description of the differential forms that satisfy  $\int d\alpha = 0$ , aside from the compactly supported case. There are, however, several choices of Stein class constructed from Hilbertian subspaces that lead to computationally tractable Stein discrepancies. One route consists in constructing a RKHS of mean-zero functions as the image of another RKHS under a Stein operator. In this case, we can use  $S_\mu$  to map a given RKHS of  $\mathbb{R}^d$ -valued functions  $\mathcal{H}$ , with (matrix-valued) reproducing kernel  $K$ , into a *Stein RKHS* of  $\mathbb{R}$ -valued functions  $S_\mu(\mathcal{H})$  associated to a *Stein reproducing kernel*  $k_\mu$ , given by (here  $q$  is the Lebesgue density of  $\mu$ )

$$k_\mu(x, y) = \frac{1}{q(x)q(y)} \partial_y \cdot \partial_x \cdot (q(x)K(x, y)q(y)).$$

The resulting Stein discrepancy can be thought of as an MMD that depends only on  $\rho$  and is known as *kernel Stein discrepancy* [203]:

$$\text{KSD}[\rho]^2 \equiv \text{MMD}[\rho \mid \mu]^2 = \int \int \frac{1}{q(x)q(y)} \partial_y \cdot \partial_x \cdot (q(x)K(x, y)q(y)) d\rho(y) d\rho(x).$$

Another class of discrepancies relies on a choice of bracket  $B$  together with a corollary from Stokes’ theorem:  $\int S_\mu^B(\alpha) d\rho = \int \alpha(X_{H-K}^{B^*}) d\rho$ , where  $e^{-H}$  and  $e^{-K}$  are the densities of  $\rho$  and  $\mu$  with respect to a common smooth measure (below the Riemannian one), while  $B^*$  is the dual bracket (the transpose of  $B$ ). We can thus re-write the Stein discrepancy as

$$\sup_{\alpha \in \mathcal{A}} \left| \int \alpha(X_{H-K}^{B^*}) d\rho \right| \tag{40}$$

over some family of 1-forms  $\mathcal{A}$ . As we did previously, we can “remove” the supremum by rewriting the above as a supremum over some unit ball of a continuous linear functional. This can be achieved once we have a Riemannian metric  $\langle \cdot, \cdot \rangle$ , which induces a natural inner product that is central to the theory of Harmonic forms, namely  $(\alpha, \beta)_\mu \equiv \int \langle \alpha, \beta \rangle d\mu$ . In particular, taking as  $\mathcal{A}$  the smooth compactly supported 1-forms in the unit ball of  $L^2(T^*\mathcal{M}, \mu)$ —the Hilbert space of square  $\mu$ -integrable 1-forms—the Stein discrepancy recovers a generalisation of the score matching [71]:

$$\text{SM}_B[\rho \mid \mu] = \int \|X_{H-K}^{B*}\|^2 d\rho = \mathbb{E}_\rho \left[ \|X_{H-K}^{B*}\|^2 \right]. \quad (41)$$

It is worth noting that, while  $L^2(T^*\mathcal{M}, \mu)$  is not a RKHS, and does not have a reproducing kernel, it remains a Hilbertian subspace of the space of de Rham currents. When  $B$  is Riemannian we recover the Riemannian score matching [21]

$$\text{SM}_G[\rho \mid \mu] = \int \|\nabla H - \nabla K\|^2 d\rho,$$

while in Euclidean space (41) yields the diffusion score matching [204].

### 4.3 Information geometry of MMDs and natural gradient descent

MMDs and Stein discrepancies have proved to be important tools in a wide range of contexts, from hypothesis testing and training generative neural networks to measuring sample quality [128, 205–209]. In the context of statistical inference, once we have chosen a suitable discrepancy,  $D$ , and a statistical model,  $\{\mu_\theta\}$ , our aim is to find the best approximation of the target distribution within the model; this corresponds to solving the optimisation problem  $\theta^* \in \arg \min_{\theta \in \Theta} D[\rho \mid \mu_\theta]$ . As mentioned previously, computing the value of the discrepancy  $D[\rho \mid \mu_\theta]$  is computationally challenging. Fortunately, we can often obtain robust Stein discrepancy estimators for smooth statistical models, whose distributions have a smooth positive Lebesgue density, as well as MMD estimators for generative model that are easy to sample from but have intractable model densities.

In either case, once we have an estimator  $\hat{D}_m$  based on  $m$  samples from the target, we must solve the approximate optimisation problem  $\theta_m^* \in \arg \min_{\theta \in \Theta} \hat{D}_m[\rho \mid \mu_\theta]$ . When the function  $\hat{D}_m[\rho \mid \mu_\theta]$  is smooth, this may be done via the accelerated Hamiltonian-based optimisation methods previously discussed (section §2). If  $D$  is a divergence function, one can also usually improve the speed of convergence by following the *natural gradient descent*, associated with the information Riemannian metric  $g_\theta$  induced by  $D$  [210–213]. In practice, this leads to implementing the update

$$\hat{\theta}_{t+1} = \hat{\theta}_t - \gamma_t \hat{g}_{\hat{\theta}_t}^{-1} \partial_{\theta_t} \hat{D}_m[\rho \mid \mu_{\hat{\theta}_t}],$$

where  $\{\gamma_t\}$  is an appropriate sequence of step sizes, and  $\hat{g}_\theta^{-1}$  is the inverse of a regularised estimate of the information tensor [214]. Finally, note that there is a deep connection between divergences and the geometric mechanics discussed in sampling and optimisation, as any divergence may be interpreted as a *discrete Lagrangian*, and hence generates a symplectic structure and integrator [215].

#### 4.3.1 Minimum Stein discrepancy estimators

When the model  $\{\mu_\theta\}$  consists of smooth measures with positive densities  $\{q_\theta\}$ , and we have access to samples  $\{x_\ell\}$  from the target, the Stein discrepancies offer a flexible family of inference methods. For SM we can use the estimator

$$\hat{\text{SM}}_m[\rho \mid \mu_\theta] = \frac{1}{m} \sum_{\ell=1}^m (\|B^T \partial_x \log q_\theta\|_2^2 + 2\partial_x \cdot (BB^T \partial_x \log q_\theta)) (x_\ell)$$



combined with the following expression for the information tensor:

$$(g_\theta)_{ij} = \int B^T \partial_x \partial_{\theta^i} \log q_\theta \cdot B^T \partial_x \partial_{\theta^j} \log q_\theta d\mu_\theta.$$

For KSD it is convenient to choose a family of matrix kernels  $K_\theta(x, y) = B_\theta(x)k(x, y)B_\theta(y)^T$ , for some scalar kernel  $k$ , and parameter-dependent matrix function  $B_\theta$ . Denoting the associated Stein reproducing kernel by  $k_{\mu_\theta, \theta}$ , we have the unbiased estimator

$$\widehat{\text{KSD}}_m[\rho] = \frac{1}{m(m-1)} \sum_{i \neq j}^m k_{\mu_\theta, \theta}(x_i, x_j),$$

and information tensor

$$(g_\theta)_{ij} = \iint (\partial_x \partial_{\theta^j} \log q_\theta)^T B_\theta(x)k(x, y)B_\theta^T(y) \partial_x \partial_{\theta^i} \log q_\theta d\mu_\theta(x) d\mu_\theta(y).$$

The parameters  $B$  and  $k$ , and the choice of statistical model, can often be adjusted to achieve characteristness, consistency, bias-robustness, and obtain central limit theorems; see [204] for details, and for numerical experiments showing an acceleration induced by the information Riemannian metric.

### 4.3.2 Likelihood-free inference with generative models

For many applications of interests, the densities of the model,  $\{\mu_\theta\}$ , cannot be evaluated or differentiated. We thus need density-free inference methods. This is the case, for instance, in the context of generative models wherein  $\mu_\theta$  is the pushforward of a distribution  $\mu$ , from which we can sample efficiently, with respect to a generator function  $T_\theta$ . Then, the minimum Stein discrepancy estimators based on KSD and SM, or other discrepancies that rely on the scores, are intractable. The MMDs are suited to this case since they depend on the target and model only through integration, which can be straightforwardly estimated using the samples. The associated information tensor is

$$(g_\theta)_{ij} = \iint \partial_\theta T_\theta(u)^T \partial_x \partial_y k(x, y)|_{(T_\theta(u), T_\theta(v))} \partial_\theta T_\theta(v) d\mu(u) d\mu(v).$$

Under appropriate choices of kernels and models one can derive theoretical guarantees, such as concentration/generalisation bounds, consistency, asymptotic normality, and robustness; see, e.g., [209, 216, 217]. Moreover, many approaches to kernel selection in a wide range of contexts have been studied, which include the median heuristic or maximising the power of hypothesis tests, and in practice mixtures of Gaussian kernels are often employed [209, 216, 218–221].

## 5 Adaptive agents through active inference

The previous sections have established some of the mathematical fundamentals of optimisation, sampling and inference. In this final section, we close with a generic use case called *active inference*. Active inference is a general framework for describing and designing adaptive agents that unifies many aspects of behaviour—including perception, planning and learning—as processes of inference. Active inference emerged in the late 2000s as a unifying theory of human brain function [82–84, 222], and has since been applied to simulate a wide range of behaviours in neuroscience [81, 223], machine learning [88, 94, 224], and robotics [85, 86]. In what follows, we derive the objective functional

overarching decision-making in active inference and describe its information geometric structure, revealing several special cases that are established notions in statistics, cognitive science and engineering. Finally, we exploit this geometric structure in a generic framework for designing adaptive agents.

## 5.1 Modelling adaptive decision-making

### 5.1.1 Behaviour, agents and environments

We define behaviour as the interaction between an agent and its environment. Together the agent and its environment form a *system* that evolves over time according to a stochastic process  $x$ . This definition entails a notion of time  $\mathcal{T}$ , which may be discrete or continuous, and a state space  $\mathcal{X}$ , which should be a measure space (e.g., discrete space, manifold, etc.). A stochastic process  $x$  is a time-indexed collection of random variables  $x_t$  on the state space. More concisely, it is a random variable over trajectories on the state space  $\mathcal{T} \rightarrow \mathcal{X}$ :

$$x : \Omega \rightarrow (\mathcal{T} \rightarrow \mathcal{X}), \omega \mapsto x(\omega) \iff x_t : \Omega \rightarrow \mathcal{X}, \omega \mapsto x(\omega)(t) \quad \forall t \in \mathcal{T}.$$

We denote by  $P$  the probability density of  $x$  on the space of paths  $\mathcal{T} \rightarrow \mathcal{X}$  with respect to a pre-specified base measure.

Typically, systems comprising an agent and its environment have three sets of states: *external* states are unknown to the agent and constitute the environment; the *observable* states are those agent's states that the agent sees but cannot directly control; finally, the *autonomous* states are those agent's states that the agent sees and can directly control. This produces a partition of the state space  $\mathcal{X}$  into states external to the agent  $\mathcal{S}$  and states belonging to the agent  $\Pi$ , which themselves comprise observable  $\mathcal{O}$  and autonomous states  $\mathcal{A}$ . As a consequence, the system  $x$  can be decomposed into external  $s$ , observable  $o$ , and autonomous  $a$  processes:

$$\mathcal{X} \equiv \mathcal{S} \times \Pi \equiv \mathcal{S} \times \mathcal{O} \times \mathcal{A} \implies x \equiv (s, \pi) \equiv (s, o, a),$$

here written as random interacting trajectories on their respective spaces (see Figure 2 for an illustration).

### 5.1.2 Decision-making in precise agents

The description of behaviour adopted so far could, in principle, describe particles interacting with a heat bath [107] as well as humans interacting with their environment (see Figure 2). We would like a description that accounts for purposeful behaviour [81, 225–229]. So what distinguishes people from small particles? An obvious distinction is that human behaviour is subject to classical as opposed to statistical mechanics. In other words, people are precise agents, with conservative dynamics.

**Definition 5.1** (Precise agent). An agent is precise when it evolves deterministically in a (possibly) stochastic environment, i.e., when  $P(\pi | s)$  is a Dirac measure for any  $s$ . For example,

$$ds_t = f(s_t, \pi_t)dt + dw_t, \quad d\pi_t = g(s_t, \pi_t)dt.$$

At any moment in time  $t$ , the agent has access, at most, to its past trajectory  $\pi_{\leq t}$ , and has agency over its future autonomous trajectory  $a_{>t}$ . We define a *decision* to be a choice of autonomous trajectory in the future given available knowledge  $a_{>t} | \pi_{\leq t}$ . We interpret  $P(s, o | \pi_{\leq t})$  as expressing the agent's *preferences* over external and observable trajectories given available data, and  $P(s, o | a_{>t}, \pi_{\leq t})$  as expressing the agent's *predictions* over external and observable paths given

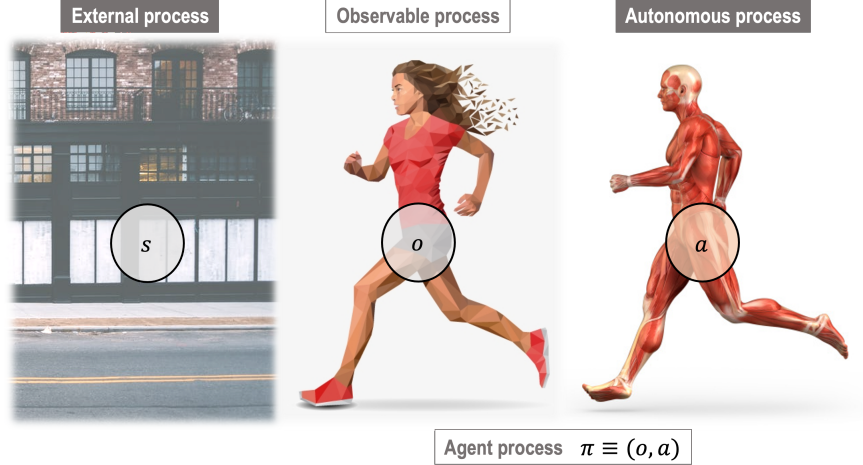


Figure 2: *Partitions and agents*. This figure illustrates a human (agent  $\pi$ ) interacting with its environment (external process  $s$ ), and the resulting partition into external  $s$ , observable  $o$ , and autonomous  $a$  processes. The external states are the environment, which the agent does not have direct access to, but which is sampled through the observable states. These could include states of the sensory epithelia (e.g., eyes and skin). The autonomous states constitute the muscles and nervous system that factor available information into decisions. In the example of human behaviour, the environment causes observations (i.e., sensations), which informs a nervous and muscular response, which in turn influences the environment. In general, autonomous responses may be informed by all past agent states  $\pi_{\leq t} = (o_{\leq t}, a_{\leq t})$  (the information available to the agent at time  $t$ ), which means that the systems we are describing are typically non-Markovian.

a decision. Crucially, decision-making in (precise) agents is a functional of the agent’s predictions and preferences<sup>10</sup>

$$\begin{aligned}
-\log P(a_{>t} | \pi_{\leq t}) &= \mathbb{E}_{P(s,o|a_{>t},\pi_{\leq t})}[-\log P(a_{>t} | \pi_{\leq t})] = \mathbb{E}[\log P(s, o | a_{>t}, \pi_{\leq t}) - \log P(s, o, a_{>t} | \pi_{\leq t})] \\
&= \mathbb{E}[\log P(s | a_{>t}, \pi_{\leq t}) - \log P(s, o | \pi_{\leq t}) + \underbrace{\log P(o | s, a_{>t}, \pi_{\leq t}) - \log P(a_{>t} | s, o, \pi_{\leq t})}_{=0}] \\
\Rightarrow -\log P(a_{>t} | \pi_{\leq t}) &= \mathbb{E}_{P(s,o|a_{>t},\pi_{\leq t})}[\log P(s | a_{>t}, \pi_{\leq t}) - \log P(s, o | \pi_{\leq t})]. \tag{EFE}
\end{aligned}$$

This functional is known as an *expected free energy* (EFE) [81, 84, 231] because it resembles the expectation of the free energy functional (a.k.a. evidence lower bound [232]) used in approximate Bayesian inference [84, 226]. We define *active inference* as Hamilton’s principle of least action on expected free energy<sup>11</sup> that expresses the most likely decision  $\mathbf{a}_{>t}$ , where

$$\mathbf{a}_{>t} \equiv \arg \min_{a_{>t}} -\log P(a_{>t} | \pi_{\leq t}). \tag{AIF}$$

### 5.1.3 The information geometry of decision-making

Interestingly, active inference (AIF) looks like it describes agents that engage in purposeful behaviour. Indeed, we can rearrange the expected free energy (EFE) in several ways, each of which reveals a fundamental trade-off that underwrites decision-making. This allows us to relate active inference to information theoretic formulations of decision-making that predominate in statistics,

<sup>10</sup>Under the precise agent assumption (Definition 5.1) it is straightforward to show that  $\mathbb{E}_{P(s,o|a_{>t},\pi_{\leq t})}[\log P(o | s, a_{>t}, \pi_{\leq t}) - \log P(a_{>t} | s, o, \pi_{\leq t})] = 0$  when the path space  $\mathcal{T} \rightarrow \mathcal{X}$  is countable [230]. Presumably, this equality can be extended to more general path spaces by a limiting argument.

<sup>11</sup>As a negative log density over paths, the expected free energy is an action in the physical sense of the word.

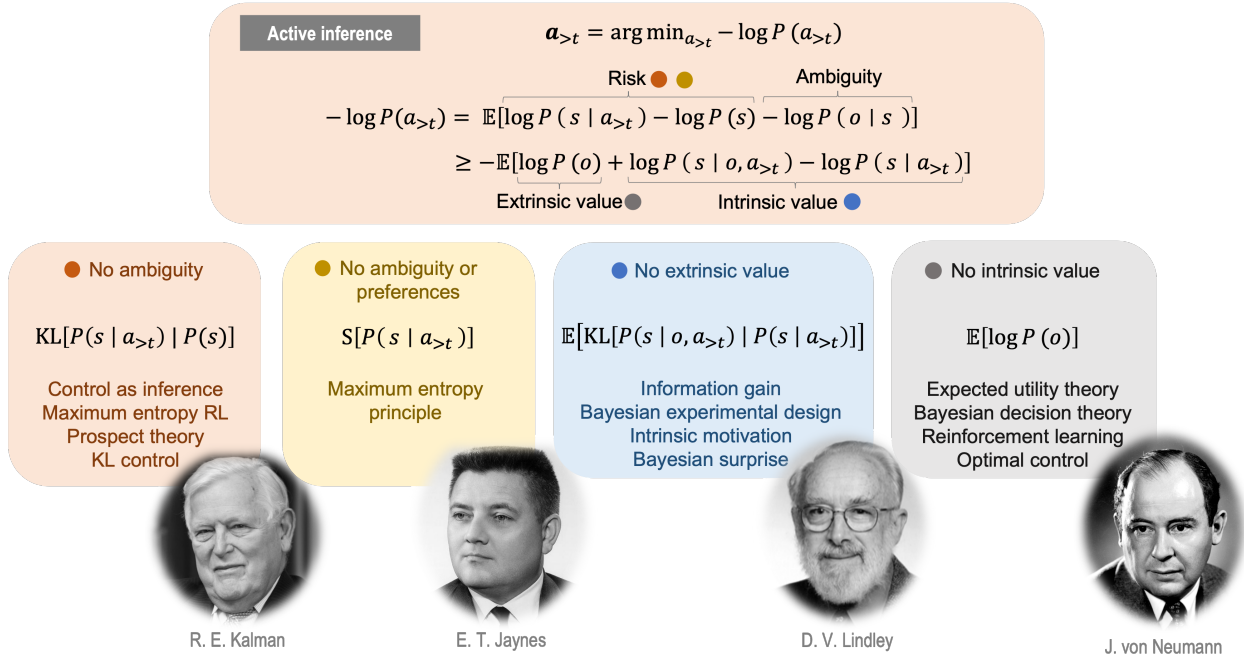


Figure 3: *Decision-making under active inference.* This figure illustrates various imperatives that underwrite decision-making under active inference in terms of several constructs that predominate in statistics, cognitive science and engineering. These formulations are disclosed when one removes certain sources of uncertainty. For example, if we remove ambiguity, decision-making minimises risk, which corresponds to aligning predictions with preferences about the external course of events. This aligns with prospect theory of human choice behaviour in economics [233] and underwrites modern approaches to control as inference [234–236], variously known as Kalman duality [237, 238], KL control [239] and maximum entropy reinforcement learning [240]. If we further remove preferences, decision-making maximises the entropy of external trajectories. This maximum entropy principle [241, 242] allows one to least commit to a pre-specified external trajectory and therefore keep options open. If we reintroduce ambiguity, but ignore preferences, decision-making maximises intrinsic value or expected information gain [243]. This underwrites Bayesian experimental design [244] and active learning in statistics [245], intrinsic motivation and artificial curiosity in machine learning and robotics [246–250]. This is mathematically equivalent to optimising expected Bayesian surprise and mutual information, which underwrites visual search [251, 252] and the organisation of our visual apparatus [253–255]. Lastly, if we remove intrinsic value, we are left with maximising extrinsic value or expected utility. This underwrites expected utility theory [78], game theory, optimal control [256, 257] and reinforcement learning [80]. Bayesian formulations of maximising expected utility under uncertainty are also known as Bayesian decision theory [77]. To ease notation, we omitted to condition every distribution in the figure by  $\pi_{\leq t}$ .

cognitive science and engineering (see Figure 3). For example, decision-making minimises both risk and ambiguity:

$$-\log P(a_{>t} | \pi_{\leq t}) = \underbrace{\text{KL} \left[ \overbrace{P(s | a_{>t}, \pi_{\leq t})}^{\text{predicted paths}} \mid \overbrace{P(s | \pi_{\leq t})}^{\text{preferred paths}} \right]}_{\text{risk}} + \underbrace{\mathbb{E}_{P(s, o | a_{>t}, \pi_{\leq t})} [ -\log P(o | s, \pi_{\leq t}) ]}_{\text{ambiguity}}. \tag{42}$$

*Risk* refers to the KL divergence between the predicted and preferred external course of events. Minimising risk entails making predicted (external) trajectories fulfil preferred external trajectories. In a nutshell, *ambiguity* refers to the expected entropy of future observations, given future external trajectories. An external trajectory that can lead to various distinct observation trajectories is highly ambiguous—and vice-versa. Thus, minimising ambiguity leads to sampling observations

that enable to recognise the external course of events. This leads to a type of observational bias commonly known as the streetlight effect [258]: when a person loses their keys at night, they initially search for them under the streetlight because the resulting observations (“I see my keys under the streetlight” or “I do not see my keys under the streetlight”) accurately disambiguate external states of affairs.

Similarly, decision-making maximises extrinsic and intrinsic value [259]:

$$\begin{aligned}
 -\log P(a_{>t} \mid \pi_{\leq t}) &= \mathbb{E}_{P(o|a_{>t}, \pi_{\leq t})} \left[ \underbrace{\text{KL} [P(s \mid o, a_{>t}, \pi_{\leq t}) \mid P(s \mid o, \pi_{\leq t})]}_{\geq 0} \right] \\
 &\quad - \underbrace{\mathbb{E}_{P(o|a_{>t}, \pi_{\leq t})} \left[ \log \overbrace{P(o \mid \pi_{\leq t})}^{\text{preferred paths}} \right]}_{\text{extrinsic value}} - \underbrace{\mathbb{E}_{P(o|a_{>t}, \pi_{\leq t})} \left[ \text{KL} [P(s \mid o, a_{>t}, \pi_{\leq t}) \mid P(s \mid a_{>t}, \pi_{\leq t})] \right]}_{\text{intrinsic value}}.
 \end{aligned}$$

*Extrinsic value* refers to the (log) likelihood of observations under the model of preferences. This corresponds to an expected utility or expected reward in behavioural economics, control theory and reinforcement learning [78, 80]. In short, maximising extrinsic value leads to sampling observations that are likely under the model of preferences. *Intrinsic value* refers to the amount of information gained about external courses of events. This measures the expected degree of belief updating about external trajectories under a decision, with versus without future observations. Making decisions to maximise information gain leads to a goal-directed form of exploration [231], driven to answer “What would happen if I did that?” [247]. Interestingly, this decision-making procedure underwrites Bayesian experimental design in statistics [244], which describes optimal experiments as those that maximise expected information gain. In summary, decision-making weighs the imperatives of maximising utility and information gain, which suggests a principled solution to the exploration-exploitation dilemma [260].

## 5.2 Realising adaptive agents

We now show how active inference affords a generic recipe to generate adaptive agents.

### 5.2.1 The basic active inference algorithm

Active inference specifies an agent by a *prediction model*  $P(s, o \mid a)$ , expressing the distribution of external and observable paths given autonomous paths, and a *preference model*  $P(s, o)$ , expressing the preferred external and observable trajectories. To aid intuition, we will refer to autonomous states as actions. At any time  $t$ , the agent knows past observations and actions  $\pi_{\leq t} = (o_{\leq t}, a_{\leq t})$ , and must make a decision  $a_{>t}$ . In discrete time, active inference proceeds by assessing the expected free energy of each possible decision and then executing the best one:

1. *Preferential inference*: infer preferences about external and observable trajectories, i.e.,

$$\text{Approximate } P(s, o \mid \pi_{\leq t}) \text{ by } Q(s, o). \tag{43}$$

2. For each possible sequence of future actions  $a_{>t}$ :

- (a) *Perceptual inference*: infer external and observable paths under the action sequence, i.e.,

$$\text{Approximate } P(s, o \mid a_{>t}, \pi_{\leq t}) \text{ by } Q(s, o \mid a_{>t}). \tag{44}$$

- (b) *Planning as inference*: assess the action sequence by evaluating its expected free energy (EFE), i.e.,

$$-\log Q(a_{>t}) \equiv \mathbb{E}_{Q(s,o|a_{>t})} [\log Q(s | a_{>t}) - \log Q(s, o)]. \quad (45)$$

3. *Decision-making*: execute the most likely decision  $\mathbf{a}_{t+1}$  according to

$$\mathbf{a}_{t+1} = \arg \max Q(a_{t+1}), \quad Q(a_{t+1}) = \sum_{a_{>t}} Q(a_{t+1} | a_{>t}) Q(a_{>t}). \quad (46)$$

### 5.2.2 Sequential decision-making under uncertainty

A common model of sequential decision-making under uncertainty is a *partially observable Markov decision process* (POMDP). A POMDP is a discrete time model of how actions influence external and observable states. In a POMDP, 1) each external state depends only on the current action and previous external state  $P(s_t | s_{t-1}, a_t)$ , and 2) each observation depends only on the current external state  $P(o_t | s_t)$ . One can additionally specify 3) a distribution of preferences over external trajectories  $P(s)$ . Together, 1) & 2) forms the agent’s (POMDP) prediction model, and 2) & 3) forms the agent’s (hidden Markov) preference model, which defines an active inference agent. A simple simulation of active inference on a POMDP is provided in Figure 4; implementation details on generic POMDPs are available in [81, 91, 261, 262]. For more complex simulations of sequential decision-making (e.g., involving hierarchical POMDPs), please see [88, 91, 223, 224, 263–265].

### 5.2.3 World model learning as inference

Due to a lack of domain knowledge, it may be challenging to specify an agent’s prediction and preference model. For example, how do external states map to observations? Should external states be represented in a discrete or continuous state space?

In active inference, generative models are learned by inferring their parameters [81, 91, 268] and structure [81, 263, 269–271]. Suppose there is an unknown parameter (or structure variable)  $m$  in the prediction model, the preference model or both. By definition, each alternative parameterisation  $m$  entails different predictions  $P(o, s | a, m)$  and preferences  $P(o, s | m)$ . Since unknowns are simply external states, we treat the parameter as an additional external state. We equip the space of parameters with a prior distribution  $P(m)$ , and define the agent with an augmented prediction (resp. preference) model that combines the different alternatives  $P(o, s, m | a) \equiv P(o, s | a, m)P(m)$  (resp.  $P(o, s, m) \equiv P(o, s | m)P(m)$ ). The parameter can then be inferred along with other external states during preferential (43) or perceptual (44) inference [81, 91, 268]. Better yet, having specified priors over parameters that are independent of actions, we can infer them separately, for example, after fixed-length sequences of decisions to reduce computational cost [81, 268].

All this says that a prior  $P(m)$  and some data  $\pi_{\leq t}$  leads to approximate posterior beliefs  $Q(m) \approx P(m | \pi_{\leq t})$  about model parameters. But what are the right priors? One way to answer this question lies in optimising a free energy functional  $F$  (a.k.a. an evidence lower bound [232]):

$$\begin{aligned} F &\equiv \underbrace{\mathbb{E}_{Q(m)} [-\log P(m, \pi_{\leq t})]}_{\text{energy}} - \underbrace{\mathbb{S} [Q(m)]}_{\text{entropy}} \\ &= \underbrace{\text{KL} [Q(m) | P(m)]}_{\text{complexity}} - \underbrace{\mathbb{E}_{Q(m)} [\log P(\pi_{\leq t} | m)]}_{\text{accuracy}}. \end{aligned}$$

Choosing priors that minimise free energy leads to parsimonious models that explain the data at hand [272]. This follows since maximising accuracy increases the likelihood of the data under

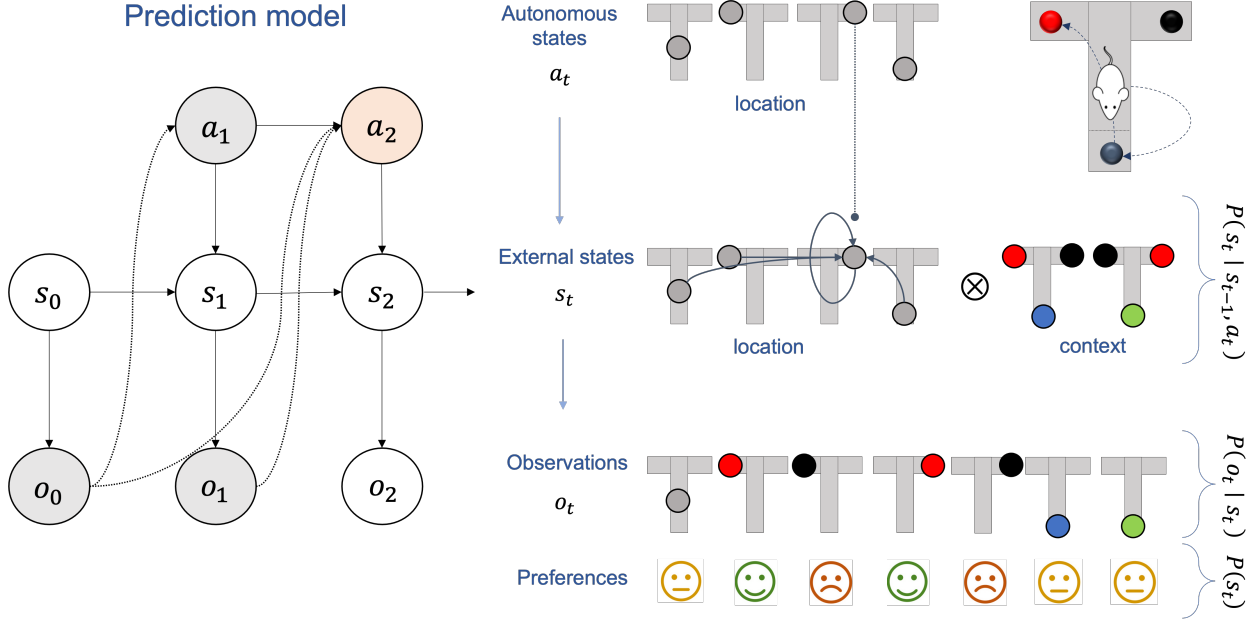


Figure 4: *Sequential decision-making in a T-Maze environment.* *Left:* The agent’s prediction model is a partially observed Markov decision process (see text) represented here as a Bayesian network [266]. The colour scheme illustrates the problem at  $t = 2$ : the agent must make a decision (in red) based on previous actions and observations (in grey), which are informative about external states and future observations (in white). *Right:*  $s_t$ : The T-Maze has four possible spatial *locations*: middle, top-left, top-right, bottom. One of the top locations contains a reward (in red), while the other contains a punishment (in black). The reward’s location determines the *context*. The bottom arm contains a cue whose colour (blue or green) discloses the context. Together, location and context determine the external state.  $o_t$ : The agent observes its spatial location. In addition, when it is at the top of the Maze, it observes the reward or the punishment; when it is at the bottom, it observes the colour of the cue.  $a_t$ : Each action corresponds to visiting one of the four spatial locations.  $P(s_t)$ : The agent prefers being at the reward’s location ( $-\log P(s_t) = +3$ ) and avoid the punishment’s location ( $-\log P(s_t) = -3$ ). All other states have a neutral preference ( $-\log P(s_t) = 0$ ).  $o_0$ : The agent is in the middle of the Maze and is unaware of the context.  $a_1$ : Visiting the bottom or top arms have a lower ambiguity than staying, as they yield observations that disclose the context. However, staying or visiting the bottom arm are safer options, as visiting a top arm risks receiving the punishment. By acting to minimise both risk and ambiguity (42) the agent goes to the bottom.  $o_1$ : The agent observes the colour of the cue and hence determines the context.  $a_2$ : All actions have equal ambiguity as the context is known. Collecting the reward has a lower risk than staying or visiting the middle, which themselves have a lower risk than collecting the punishment. Thus, the agent visits the arm with the reward. See [267] for more details.

the posterior model, while minimising complexity decreases the movement from prior to posterior, which can be seen as a proxy for computational cost. Maximising accuracy usually results in generative models involving universal function approximators [88, 224, 264], while minimising complexity results in organising representations in sparse, compartmentalised and hierarchical generative models [263, 270, 271], where higher levels of the hierarchy encode more abstract representations and vice-versa [265]. A computationally efficient method to compare priors by their free energy is Bayesian model reduction [81, 273]. In conclusion, free energy unifies inference and model selection under a single objective function.

### 5.2.4 Scaling active inference

We conclude by identifying promising scaling methods for active inference that enable computationally tractable implementations in a variety of applications.

Planning for all possible courses of action is computationally expensive as the number of action sequences is exponential in the length of the sequence. One way to finesse this is by planning only for intelligently chosen subsets of action sequences, using sampling algorithms such as Monte-Carlo tree search [87, 224, 274–276]. Monte-Carlo sampling can also be used to finesse the expectations inherent in assessing action sequences (45) [224]. A complementary approach is to assess actions, instead of action sequences, by conditioning future actions to be optimal in the sense that they minimise the expected free energy [228, 277]. This idea leads to a backward form of planning, where the agent plans for the best action at the last time-step, followed by the best action at the penultimate time-step, and so on, until the present. Crucially, it leads to smarter agents [228, 277] whose computational complexity scales linearly (as opposed to exponentially) in the length of action sequences [278].

Scalable inference methods [279] can be used to make active inference more efficient [280]. For example, we can train neural networks to predict the various posterior distributions, including the posterior over actions [88, 224, 281]. While training, the output of the neural network can be used as an initial conditions for variational inference [282], resulting in accurate inferences whose computational cost decrease as the network learns. Additionally, optimising free energy reduces to efficient *message passing* schemes, when one imposes certain simplifying restrictions to the family of candidate distributions [283–287].

A much cheaper implementation of active inference exists for continuous states evolving in continuous time. The method frames perception and decision-making as variational inference, by simulating a gradient flow on free energy in an extended state space [82, 226]. Furthermore, it can be combined with discrete active inference to operate efficiently in generative models combining discrete and continuous states [288]. As an example, high-dimensional observations in the continuous domain (e.g., speech) processed through continuous active inference are converted into discrete, abstract representations (e.g., semantics) [281]. Based on these representations, the agent makes high-level, categorical decisions (e.g., “I want to move over there”), which contextualise low-level, continuous actions (e.g., the continuous motion of a limb towards the goal location) [289].

## Acknowledgements

The authors thank Noor Sajid, Samuel Tenka, Zafeiros Fountas and Panagiotis Tigas for helpful discussions on adaptive agents. LD is supported by the Fonds National de la Recherche, Luxembourg (Project code: 13568875). KF is supported by funding for the Wellcome Centre for Human Neuroimaging (Ref: 205103/Z/16/Z) and a Canada-UK Artificial Intelligence Initiative (Ref: ES/T01279X/1). GAP was partially supported by JPMorgan Chase & Co under J.P. Morgan A.I. Research Awards in 2019 and 2021 and by the EPSRC, grant number EP/P031587/1. This publication is based on work partially supported by the EPSRC Centre for Doctoral Training in Mathematics of Random Systems: Analysis, Modelling and Simulation (EP/S023925/1). AB, GF, MG and MIJ thank the support of the Army Research Office (ARO) under contract W911NF-17-1-0304 as part of the collaboration between US DOD, UK MOD and UK Engineering and Physical Research Council (EPSRC) under the Multidisciplinary University Research Initiative (MURI).

## References

- [1] R. I. McLachlan and G. R. W. Quispel. Splitting methods. *Acta Numer.*, 11:341, 2002.



- [2] E. Hairer, C. Lubich, and G. Wanner. *Geometric Numerical Integration: Structure-Preserving Algorithms for Ordinary Differential Equations*. Springer, 2010.
- [3] B. Leimkuhler and S. Reich. *Simulating Hamiltonian Dynamics*. Cambridge University Press, 2004.
- [4] E. Celledoni, H. Marthinsen, and B. Owren. An introduction to Lie group integrators: basics, new developments and applications. *J. Comput. Phys.*, 257:1040–1061, 2014.
- [5] J. E. Marsden and M. West. Discrete mechanics and variational integrators. *Acta Numer.*, 10:357–514, 2001.
- [6] M. Betancourt, M. I. Jordan, and A. Wilson. On symplectic optimization. 2018. arXiv:1802.03653 [stat.CO].
- [7] A. Bravetti, M. L. Daza-Torres, H. Flores-Arguedas, and M. Betancourt. Optimization algorithms inspired by the geometry of dissipative systems. 2019. arXiv:1912.02928 [math.OC].
- [8] G. França, J. Sulam, D. P. Robinson, and R. Vidal. Conformal symplectic and relativistic optimization. *J. Stat. Mech.*, 2020(12):124008, 2020.
- [9] G. França, M. I. Jordan, and R. Vidal. On dissipative symplectic integration with applications to gradient-based optimization. *J. Stat. Mech.*, 2021(4):043402, 2021.
- [10] G. França, A. Barp, M. Girolami, and M. I. Jordan. Optimization on manifolds: A symplectic approach. 2021. arXiv:2107.11231 [cond-mat.stat-mech].
- [11] F. Alimisis, A. Orvieto, G. Becigneul, and A. Lucchi. Momentum improves optimization on Riemannian manifolds. *Int. Conf. Artificial Intelligence and Stats.*, 130:1351–1359, 2021.
- [12] M. Rousset, G. Stoltz, and T. Lelièvre. *Free Energy Computations: A Mathematical Perspective*. World Scientific, 2010.
- [13] S. Duane, A.D. Kennedy, B. J. Pendleton, and D. Roweth. Hybrid Monte Carlo. *Phys. Lett. B*, 195(2):216–222, 1987.
- [14] M. Betancourt, S. Byrne, S. Livingstone, and M. Girolami. The geometric foundations of Hamiltonian Monte Carlo. *Bernoulli*, 23(4A):2257–2298, 2017.
- [15] S. Livingstone, M. Betancourt, S. Byrne, and M. Girolami. On the geometric ergodicity of Hamiltonian Monte Carlo. *Bernoulli*, 25(4A):3109–3138, 2019.
- [16] A. Barp, A. Kennedy, and M. Girolami. Hamiltonian Monte Carlo on symmetric and homogeneous spaces via symplectic reduction. 2019.
- [17] E. Celledoni, M. J. Ehrhardt, C. Etmann, R. I. McLachlan, B. Owren, C. B. Schonlieb, and F. Sherry. Structure-preserving deep learning. *Eur. J. Applied Math.*, 32(5):888–936, 2021.
- [18] M. M. Bronstein, J. Bruna, T. Cohen, and P. Velickovic. Geometric deep learning: Grids, groups, graphs, geodesics, and gauges, 2021. arXiv:2104.13478 [cs.LG].
- [19] M. Vaillant and J. Glaunes. Surface matching via currents. In *Biennial Int. Conf. Information Processing in Medical Imaging*, pages 381–392. Springer, 2005.
- [20] S. Durrleman, X. Pennec, A. Trounev, and N. Ayache. Statistical models of sets of curves and surfaces based on currents. *Medical Image Analysis*, 13(5):793–808, 2009.
- [21] A. Barp, Chris J. Oates, E. Porcu, and M. Girolami. A Riemann-Stein Kernel Method. 2020. arXiv:1810.04946 [math, stat].
- [22] P. Harms, P. W. Michor, X. Pennec, and S. Sommer. Geometry of sample spaces. 2020. arXiv:2010.08039.
- [23] C. R. Rao. Information and the accuracy attainable in the estimation of statistical parameters. In *Breakthroughs in Statistics*, pages 235–247. Springer, 1992.
- [24] H. Jeffreys. An invariant form for the prior probability in estimation problems. *Proc. Royal Soc. London. Series A. Math. and Phys. Sci.*, 186(1007):453–461, 1946.
- [25] S. Amari. *Information geometry and its applications*, volume 194. Springer, 2016.
- [26] N. Ay, J. Jost, H. Vân Lê, and L. Schwachhöfer. *Information geometry*, volume 64. Springer, 2017.
- [27] F. Nielsen. An elementary introduction to information geometry. *Entropy*, 22(10):1100, 2020.
- [28] S. Amari. *Differential-geometrical methods in statistics*, volume 28. Springer Science & Business Media, 2012.
- [29] N. N. Chentsov. Categories of mathematical statistics. *Uspekhi Matematicheskikh Nauk*, 20(4):194–195, 1965.
- [30] J. Jost, H. V. Lê, and T. D. Tran. Probabilistic morphisms and bayesian nonparametrics. *Eur. Phys. J. Plus*, 136(4):1–29, 2021.
- [31] B. T. Polyak. Some methods of speeding up the convergence of iteration methods. *USSR Comp. Math. and Math. Phys.*, 4(5):1–17, 1964.
- [32] Y. Nesterov. A method of solving a convex programming problem with convergence rate  $O(1/k^2)$ . *Soviet Math. Doklady*, 27(2):372–376, 1983.
- [33] W. Su, S. Boyd, and E. J. Candès. A differential equation for modeling Nesterov’s accelerated gradient method: Theory and insights. *J. Mach. Learn. Res.*, 17(153):1–43, 2016.
- [34] A. Wibisono, A. C. Wilson, and M. I. Jordan. A variational perspective on accelerated methods in optimization. *Proc. Nat. Acad. Sci.*, 113(47):E7351–E7358, 2016.
- [35] A. Wilson, B. Recht, and M. I. Jordan. A Lyapunov analysis of accelerated methods in optimization. *J. Mach. Learn. Res.*, 22:1–34, 2021.

- [36] G. Franca, D. Robinson, and R. Vidal. ADMM and accelerated ADMM as continuous dynamical systems. 80:1559–1567, 2018.
- [37] G. França, D. P. Robinson, and R. Vidal. A nonsmooth dynamical systems perspective on accelerated extensions of ADMM. 2018. arXiv:1808.04048 [math.OC].
- [38] G. França, D. P. Robinson, and R. Vidal. Gradient flows and proximal splitting methods: A unified view on accelerated and stochastic optimization. *Phys. Rev. E*, 103:053304, 2021.
- [39] M. Muehlebach and M. I. Jordan. Optimization with momentum: Dynamical, control-theoretic, and symplectic perspectives. *J. Mach. Learn. Res.*, 22(73):1–50, 2021.
- [40] M. Muehlebach and M. I. Jordan. On constraints in first-order optimization: A view from non-smooth dynamical systems. 2021. arXiv:2107.08225, [math.OC].
- [41] M. Takahashi and M. Imada. Monte Carlo calculation of quantum systems. II. Higher order correction. *J. Phys. Soc. Jpn.*, 53:3765—3769, 1984.
- [42] M. Suzuki. Fractal decomposition of exponential operators with applications to many-body theories and Monte Carlo simulations. *Phys. Lett. A*, 146:319–323, 1990.
- [43] H. Yoshida. Construction of higher order symplectic integrators. *Phys. Lett. A*, 150(5):262–268, 1990.
- [44] J. M. Sanz-Serna. Symplectic integrators for Hamiltonian problems: An overview. *Acta Numerica*, 1:243–286, 1992.
- [45] G. Benettin and A. Giorgilli. On the Hamiltonian interpolation of near-to-the-identity symplectic mappings with application to symplectic integration algorithms. *J. Stat. Phys.*, 74:1117–1143, 1994.
- [46] R. I. McLachlan and G. R. W. Quispel. Geometric integrators for ODEs. *J. Phys. A: Math. Gen.*, 39:5251–5285, 2006.
- [47] E. Forest. Geometric integration for particle accelerators. *J. Phys. A: Math. Gen.*, 39:5321—5377, 2006.
- [48] A. D. Kennedy, P. J. Silva, and M. A. Clark. Shadow Hamiltonians, Poisson brackets, and gauge theories. *Phys. Rev. D*, 87:034511, 2013.
- [49] R. M. Neal. MCMC using Hamiltonian dynamics. In *Handbook of Markov Chain Monte Carlo*. Chapman and Hall/CRC, 2011.
- [50] F. Otto. The geometry of dissipative evolution equations: the porous medium equation. *Comm. Partial Differential Equations*, 26:101–174, 2001.
- [51] R. Jordan, D. Kinderlehrer, and F. Otto. The variational formulation of the Fokker-Planck equation. *SIAM J. Math. Anal.*, 29(1):1–17, 1998.
- [52] R. M. Neal. Slice sampling. *The annals of statistics*, 31(3):705–767, 2003.
- [53] I. Murray, R. Adams, and D. MacKay. Elliptical slice sampling. In *Int. Conf. Artificial Intelligence and Stats.*, pages 541–548. JMLR Workshop and Conference Proceedings, 2010.
- [54] Mark HA Davis. Piecewise-deterministic markov processes: A general class of non-diffusion stochastic models. *Journal of the Royal Statistical Society: Series B (Methodological)*, 46(3):353–376, 1984.
- [55] A. Bouchard-Côté, S. J. Vollmer, and A. Doucet. The bouncy particle sampler: A nonreversible rejection-free markov chain monte carlo method. *J. Amer. Stats. Assoc.*, 113(522):855–867, 2018.
- [56] P. Vanetti, A. Bouchard-Côté, G. Deligiannidis, and A. Doucet. Piecewise-deterministic Markov Chain Monte Carlo. 2017. arXiv:1707.05296.
- [57] J. Bierkens, P. Fearnhead, and G. Roberts. The zig-zag process and super-efficient sampling for Bayesian analysis of big data. *Ann. Stats.*, 47(3):1288–1320, 2019.
- [58] J. Bierkens and G. Roberts. A piecewise deterministic scaling limit of lifted metropolis–hastings in the curie–weiss model. *Ann. App. Prob.*, 27(2):846–882, 2017.
- [59] E. A. J. F. Peters and G. de With. Rejection-free monte carlo sampling for general potentials. *Phys. Rev. E*, 85(2):026703, 2012.
- [60] G. O. Roberts and R. L. Tweedie. Exponential convergence of Langevin distributions and their discrete approximations. *Bernoulli*, pages 341–363, 1996.
- [61] A. Durmus and E. Moulines. Nonasymptotic convergence analysis for the unadjusted Langevin algorithm. *Ann. App. Prob.*, 27(3):1551–1587, 2017.
- [62] A. Durmus, E. Moulines, and M. Pereyra. Efficient bayesian computation by proximal markov chain monte carlo: when langevin meets moreau. *SIAM J. on Imaging Sci.*, 11(1):473–506, 2018.
- [63] A. Garbuno-Inigo, F. Hoffmann, W. Li, and A. M. Stuart. Interacting Langevin diffusions: gradient structure And ensemble Kalman sampler. 2019. arXiv:1903.08866 [math].
- [64] M. Betancourt. A conceptual introduction to hamiltonian monte carlo. 2017. arXiv:1701.02434.
- [65] A. Barp, F-X. Briol, A. D. Kennedy, and M. Girolami. Geometry and dynamics for Markov Chain Monte Carlo. *Annual Rev. Stats. and its App.*, 5:451–471, 2018.
- [66] N. R. Metropolis, A. W. Rosenbluth, M. N. Rosenbluth, A. H. Teller, and E. Teller. Equation of state calculations by fast computing machines. *J. Chem. Phys.*, 21(6):1087–1092, 1953.

- [67] W. K. Hastings. *Monte Carlo Sampling Methods Using Markov Chains and their Applications*. Oxford University Press, 1970.
- [68] B. J. Alder and T. E. Wainwright. Studies in molecular dynamics. I. general method. *J. Chem. Phys.*, 31(2):459–466, 1959.
- [69] A. W. Van der Vaart. *Asymptotic Statistics*, volume 3. Cambridge university press, 2000.
- [70] V. Vapnik. *The Nature of Statistical Learning Theory*. Springer Science & Business Media, 1999.
- [71] A. Hyvärinen and P. Dayan. Estimation of non-normalized statistical models by score matching. *J. Mach. Learn. Res.*, 6(4), 2005.
- [72] M. Parry, A. P. Dawid, and S. Lauritzen. Proper local scoring rules. *Ann. Stats.*, 40(1):561–592, 2012.
- [73] C. Villani. *Optimal Transport: Old and New*. Springer, 2009.
- [74] F. Bassetti, A. Bodini, and E. Regazzini. On minimum Kantorovich distance estimators. *Stats. & Prob. Lett.*, 76(12):1298–1302, 2006.
- [75] G. Peyré, M. Cuturi, et al. Computational optimal transport: With applications to data science. *Found. Trends Mach. Learn.*, 11(5-6):355–607, 2019.
- [76] M. Cuturi. Sinkhorn distances: Lightspeed computation of optimal transport. *NeurIPS*, 26:2292–2300, 2013.
- [77] J. O. Berger. *Statistical Decision Theory and Bayesian Analysis*. Springer Series in Statistics. Springer-Verlag, New York, second edition, 1985.
- [78] J. Von Neumann and O. Morgenstern. *Theory of Games and Economic Behavior*. Princeton University Press, 1944.
- [79] R. E. Bellman and S. E. Dreyfus. *Applied Dynamic Programming*. Princeton University Press, 2015.
- [80] A. Barto and R. Sutton. *Reinforcement Learning: An Introduction*. A Bradford Book, 1992.
- [81] L. Da Costa, T. Parr, N. Sajid, S. Veselic, V. Neacsu, and K. Friston. Active inference on discrete state-spaces: A synthesis. *J. Math. Psychology*, 99:102447, 2020.
- [82] K. J. Friston, J. Daunizeau, J. Kilner, and S. J. Kiebel. Action and behavior: A free-energy formulation. *Biological Cybernetics*, 102(3):227–260, 2010.
- [83] K. Friston. The free-energy principle: A unified brain theory? *Nature Reviews Neuroscience*, 11(2):127–138, 2010.
- [84] Karl Friston, Francesco Rigoli, Dimitri Ognibene, Christoph Mathys, Thomas Fitzgerald, and Giovanni Pezzulo. Active inference and epistemic value. *Cognitive Neuroscience*, 6(4):187–214, October 2015.
- [85] Pablo Lanillos, Cristian Meo, Corrado Pezzato, Ajith Anil Meera, Mohamed Baioumy, Wataru Ohata, Alexander Tschantz, Beren Millidge, Martijn Wisse, Christopher L. Buckley, and Jun Tani. Active Inference in Robotics and Artificial Agents: Survey and Challenges. *arXiv:2112.01871 [cs]*, December 2021.
- [86] Lancelot Da Costa, Pablo Lanillos, Noor Sajid, Karl Friston, and Shujhat Khan. How Active Inference Could Help Revolutionise Robotics. *Entropy*, 24(3):361, March 2022.
- [87] David Silver, Aja Huang, Chris J. Maddison, Arthur Guez, Laurent Sifre, George van den Driessche, Julian Schrittwieser, Ioannis Antonoglou, Veda Panneershelvam, Marc Lanctot, Sander Dieleman, Dominik Grewe, John Nham, Nal Kalchbrenner, Ilya Sutskever, Timothy Lillicrap, Madeleine Leach, Koray Kavukcuoglu, Thore Graepel, and Demis Hassabis. Mastering the game of Go with deep neural networks and tree search. *Nature*, 529(7587):484–489, 2016.
- [88] B. Millidge. Deep active inference as variational policy gradients. *J. Math. Psychology*, 96:102348, 2020.
- [89] O. van der Himst and P. Lanillos. Deep Active Inference for Partially Observable MDPs. 2020. *arXiv:2009.03622 [cs, stat]*.
- [90] Maell Cullen, Ben Davey, Karl J. Friston, and Rosalyn J. Moran. Active Inference in OpenAI Gym: A Paradigm for Computational Investigations Into Psychiatric Illness. *Biological Psychiatry: Cognitive Neuroscience and Neuroimaging*, 3(9):809–818, September 2018.
- [91] Noor Sajid, Philip J. Ball, Thomas Parr, and Karl J. Friston. Active Inference: Demystified and Compared. *Neural Computation*, 33(3):674–712, January 2021.
- [92] Dimitrije Marković, Hrvoje Stojić, Sarah Schwöbel, and Stefan J. Kiebel. An empirical evaluation of active inference in multi-armed bandits. *Neural Networks*, 144:229–246, December 2021.
- [93] Aswin Paul, Noor Sajid, Manoj Gopalkrishnan, and Adeel Razi. Active Inference for Stochastic Control. *arXiv:2108.12245 [cs]*, August 2021.
- [94] Pietro Mazzaglia, Tim Verbelen, and Bart Dhoedt. Contrastive Active Inference. In *Advances in Neural Information Processing Systems*, May 2021.
- [95] A. C. Hansen. A theoretical framework for backward error analysis on manifolds. *J. Geom. Mech.*, 3(1):81–111, 2011.
- [96] R. I. McLachlan, G R. W. Quispel, and N. Robidoux. Geometric integration using discrete gradients. *Philosophical Transactions of the Royal Society of London. Series A: Mathematical, Physical and Engineering Sciences*, 357(1754):1021–1045, 1999.
- [97] R. McLachlan and M. Perlmutter. Conformal Hamiltonian systems. *J. Geom. and Phys.*, 39:276–300, 2001.

- [98] H. Marthinsen and B. Owren. Geometric integration of non-autonomous Hamiltonian problems. *Adv. Comput. Math.*, 42:313–332, 2016.
- [99] M. Asorey, J. F. Carinena, and L. A. Ibort. Generalized canonical transformations for time-dependent systems. *J. Math. Phys.*, 24(12):2745–2750, 1983.
- [100] H. C. Andersen. Rattle: A “velocity” version of the shake algorithm for molecular dynamics calculations. *J. Comput. Phys.*, 52(1):24–34, 1983.
- [101] B. J. Leimkuhler and R. D. Skeel. Symplectic numerical integrators in constrained Hamiltonian systems. *J. Comput. Phys.*, 112:117–125, 1994.
- [102] R. I. McLachlan, K. Modin, O. Verdier, and M. Wilkins. Geometric generalizations of SHAKE and RATTLE. *Found. Comput. Math.*, (14):339–370, 2014.
- [103] B. Leimkuhler and C. Matthews. Efficient molecular dynamics using geodesic integration and solvent-solute splitting. *Proc. Royal Soc. A: Math., Phys. and Eng. Sci.*, 472(2189):20160138, 2016.
- [104] H. Zhang and S. Sra. First-order methods for geodesically convex optimization. *Conf. Learning Theory*, pages 1617–1638, 2016.
- [105] Luigi Ambrosio, Nicola Gigli, and Giuseppe Savare. *Gradient Flows: In Metric Spaces and in the Space of Probability Measures*. Springer Science & Business Media, January 2005.
- [106] Michela Ottobre. Markov Chain Monte Carlo and Irreversibility. *Reports on Mathematical Physics*, 77:267–292, June 2016.
- [107] Grigorios A. Pavliotis. *Stochastic Processes and Applications: Diffusion Processes, the Fokker-Planck and Langevin Equations*. Number volume 60 in Texts in Applied Mathematics. Springer, New York, 2014.
- [108] Cédric Villani. *Hypoconvexity*, volume 202 of *Memoirs of the American Mathematical Society*. American Mathematical Society, November 2009.
- [109] Yi-An Ma, Niladri Chatterji, Xiang Cheng, Nicolas Flammarion, Peter Bartlett, and Michael I. Jordan. Is there an analog of nesterov acceleration for mcmc?, 2019.
- [110] D. J. C. MacKay. *Information theory, inference and learning algorithms*. Cambridge university press, 2003.
- [111] Martin Hairer. Ergodic Properties of Markov Processes. 2018.
- [112] Alessandro Barp, So Takao, Michael Betancourt, Alexis Arnaudon, and Mark Girolami. A Unifying and Canonical Description of Measure-Preserving Diffusions. *arXiv:2105.02845 [math, stat]*, May 2021.
- [113] Lars Hörmander. Hypoelliptic second order differential equations. *Acta Mathematica*, 119:147–171, 1967.
- [114] J.M. Bismut. Martingales, the malliavin calculus and hypoellipticity under general hörmander’s conditions. *Zeitschrift für Wahrscheinlichkeitstheorie und verwandte Gebiete*, 56(4):469–505, 1981.
- [115] Yi-An Ma, Tianqi Chen, and Emily B. Fox. A Complete Recipe for Stochastic Gradient MCMC. *arXiv:1506.04696 [math, stat]*, October 2015.
- [116] Chii-Ruey Hwang, Shu-Yin Hwang-Ma, and Shuenn-Jyi Sheu. Accelerating diffusions. *The Annals of Applied Probability*, 15(2):1433–1444, May 2005.
- [117] Djilil Chafaï. Entropies, convexity, and functional inequalities, On  $\Phi$ -entropies and  $\Phi$ -Sobolev inequalities. *Journal of Mathematics of Kyoto University*, 44(2):325–363, January 2004.
- [118] Aldéric Joulin and Yann Ollivier. Curvature, concentration and error estimates for Markov chain Monte Carlo. *The Annals of Probability*, 38(6):2418–2442, November 2010.
- [119] Luc Rey-Bellet and Kostantinos Spiliopoulos. Irreversible Langevin samplers and variance reduction: A large deviation approach. *Nonlinearity*, 28(7):2081–2103, July 2015.
- [120] A. B. Duncan, T. Lelièvre, and G. A. Pavliotis. Variance Reduction Using Nonreversible Langevin Samplers. *Journal of Statistical Physics*, 163(3):457–491, May 2016.
- [121] U. G. Haussmann and E. Pardoux. Time Reversal of Diffusions. *Annals of Probability*, 14(4):1188–1205, October 1986.
- [122] Radford M. Neal. Improving Asymptotic Variance of MCMC Estimators: Non-reversible Chains are Better. *arXiv:math/0407281*, July 2004.
- [123] Tony Lelièvre, Francis Nier, and Grigorios A. Pavliotis. Optimal non-reversible linear drift for the convergence to equilibrium of a diffusion. *Journal of Statistical Physics*, 152(2):237–274, July 2013.
- [124] Sheng-Jih Wu, Chii-Ruey Hwang, and Moody T. Chu. Attaining the Optimal Gaussian Diffusion Acceleration. *Journal of Statistical Physics*, 155:571–590, May 2014.
- [125] Benjamin J. Zhang, Youssef M. Marzouk, and Konstantinos Spiliopoulos. Geometry-informed irreversible perturbations for accelerated convergence of Langevin dynamics. *arXiv:2108.08247 [math, stat]*, August 2021.
- [126] Antonietta Mira. Ordering and Improving the Performance of Monte Carlo Markov Chains. *Statistical Science*, 16(4):340–350, November 2001.
- [127] M. Girolami and B. Calderhead. Riemann manifold langevin and hamiltonian monte carlo methods. *Journal of the Royal Statistical Society: Series B (Statistical Methodology)*, 73(2):123–214, 2011.

- [128] Assyr Abdulle, Grigorios A. Pavliotis, and Gilles Vilmart. Accelerated convergence to equilibrium and reduced asymptotic variance for Langevin dynamics using Stratonovich perturbations. *Comptes Rendus Mathématique*, 357(4):349–354, April 2019.
- [129] Bernard Helffer. Remarks on Decay of Correlations and Witten Laplacians Brascamp–Lieb Inequalities and Semiclassical Limit. *Journal of Functional Analysis*, 155(2):571–586, June 1998.
- [130] Adrien Saumard and Jon A. Wellner. Log-concavity and strong log-concavity: A review. *Statistics Surveys*, 8(none):45–114, January 2014.
- [131] Arnaud Guillin and Pierre Monmarché. Optimal linear drift for the speed of convergence of an hypoelliptic diffusion. *arXiv:1604.07295 [math]*, October 2021.
- [132] Yi-An Ma, Niladri Chatterji, Xiang Cheng, Nicolas Flammarion, Peter Bartlett, and Michael I. Jordan. Is There an Analog of Nesterov Acceleration for MCMC? *arXiv:1902.00996 [cs, math, stat]*, October 2019.
- [133] Martin Chak, Nikolas Kantas, Tony Lelièvre, and Grigorios A Pavliotis. Optimal friction matrix for underdamped Langevin sampling. November 2021.
- [134] A. B. Duncan, N. Nüsken, and G. A. Pavliotis. Using Perturbed Underdamped Langevin Dynamics to Efficiently Sample from Probability Distributions. *Journal of Statistical Physics*, 169(6):1098–1131, December 2017.
- [135] J. C. Mattingly, A. M. Stuart, and D. J. Higham. Ergodicity for SDEs and approximations: Locally Lipschitz vector fields and degenerate noise. *Stochastic Processes and their Applications*, 101(2):185–232, October 2002.
- [136] Markos Katsoulakis, Yannis Pantazis, and Luc Rey-Bellet. Measuring the Irreversibility of Numerical Schemes for Reversible Stochastic Differential Equations. *ESAIM: Mathematical Modelling and Numerical Analysis - Modélisation Mathématique et Analyse Numérique*, 48(5):1351–1379, 2014.
- [137] Jonathan C. Mattingly, Andrew M. Stuart, and M. V. Tretyakov. Convergence of Numerical Time-Averaging and Stationary Measures via Poisson Equations. *SIAM Journal on Numerical Analysis*, 48(2):552–577, January 2010.
- [138] T. Radivojević, M. Fernández-Pendás, J. M. Sanz-Serna, and E. Akhmatkaya. Multi-stage splitting integrators for sampling with modified hamiltonian monte carlo methods. *Journal of Computational Physics*, 373:900–916, 2018.
- [139] R. M. Neal. Bayesian training of backpropagation networks by the hybrid monte carlo method. Technical report, Citeseer, 1992.
- [140] Eric Cances, Frédéric Legoll, and Gabriel Stoltz. Theoretical and numerical comparison of some sampling methods for molecular dynamics. *ESAIM: Mathematical Modelling and Numerical Analysis*, 41(2):351–389, 2007.
- [141] Youhan Fang, Jesus-Maria Sanz-Serna, and Robert D Skeel. Compressible generalized hybrid monte carlo. *The Journal of chemical physics*, 140(17):174108, 2014.
- [142] A. Barp. The bracket geometry of statistics. 2020.
- [143] A. Weinstein. The modular automorphism group of a poisson manifold. *Journal of Geometry and Physics*, 23(3-4):379–394, 1997.
- [144] D. D. Holm, J. E. Marsden, and T. S. Ratiu. The euler–poincaré equations and semidirect products with applications to continuum theories. *Advances in Mathematics*, 137(1):1–81, 1998.
- [145] K. Modin, M. Perlmutter, S. Marsland, and R. McLachlan. Geodesics on lie groups: Euler equations and totally geodesic subgroup. 2010.
- [146] A. Barp. Hamiltonian monte carlo on lie groups and constrained mechanics on homogeneous manifolds. In *International Conference on Geometric Science of Information*, pages 665–675. Springer, 2019.
- [147] A. Holbrook, S. Lan, A. Vandenberg-Rodes, and B. Shahbaba. Geodesic lagrangian monte carlo over the space of positive definite matrices: with application to bayesian spectral density estimation. *Journal of statistical computation and simulation*, 88(5):982–1002, 2018.
- [148] A. Holbrook, A. Vandenberg-Rodes, and B. Shahbaba. Bayesian inference on matrix manifolds for linear dimensionality reduction. *arXiv preprint arXiv:1606.04478*, 2016.
- [149] T. Lelièvre, M. Rousset, and G. Stoltz. Hybrid Monte Carlo methods for sampling probability measures on submanifolds. *Numerische Mathematik*, 143(2):379–421, 2019.
- [150] T. Lelièvre, G. Stoltz, and W. Zhang. Multiple projection mcmc algorithms on submanifolds. *arXiv preprint arXiv:2003.09402*, 2020.
- [151] M. M. Graham, A. H. Thiery, and A. Beskos. Manifold markov chain monte carlo methods for bayesian inference in a wide class of diffusion models. *arXiv preprint arXiv:1912.02982*, 2019.
- [152] K. X. Au, M. M. Graham, and A. H. Thiery. Manifold lifting: scaling mcmc to the vanishing noise regime. *arXiv preprint arXiv:2003.03950*, 2020.
- [153] S. Livingstone and M. Girolami. Information-geometric markov chain monte carlo methods using diffusions. *Entropy*, 16(6):3074–3102, 2014.
- [154] M. Tao. Explicit symplectic approximation of nonseparable hamiltonians: Algorithm and long time performance. *Physical Review E*, 94(4):043303, 2016.

- [155] . D. Cobb, A. G. Baydin, A. Markham, and S. J. Roberts. Introducing an explicit symplectic integration scheme for riemannian manifold hamiltonian monte carlo. *arXiv preprint arXiv:1910.06243*, 2019.
- [156] C. Predescu, R. A. Lippert, M. P. Eastwood, D. Ierardi, H. Xu, M. Jensen, K. J. Bowers, J. Gullingsrud, C. A. Rendleman, R. O. Dror, et al. Computationally efficient molecular dynamics integrators with improved sampling accuracy. *Molecular Physics*, 110(9-10):967–983, 2012.
- [157] S. Blanes, F. Casas, and J. M. Sanz-Serna. Numerical integrators for the hybrid monte carlo method. *SIAM Journal on Scientific Computing*, 36(4):A1556–A1580, 2014.
- [158] M. Fernández-Pendás, E. Akhmatskaya, and J. M. Sanz-Serna. Adaptive multi-stage integrators for optimal energy conservation in molecular simulations. *Journal of Computational Physics*, 327:434–449, 2016.
- [159] C. M. Campos and J. M. Sanz-Serna. Palindromic 3-stage splitting integrators, a roadmap. *Journal of Computational Physics*, 346:340–355, 2017.
- [160] N. Bou-Rabee and J. M. Sanz-Serna. Geometric integrators and the hamiltonian monte carlo method. *Acta Numerica*, 27:113–206, 2018.
- [161] M. A. Clark, B. Joó, A. D. Kennedy, and P. J. Silva. Improving dynamical lattice qcd simulations through integrator tuning using poisson brackets and a force-gradient integrator. *Physical Review D*, 84(7):071502, 2011.
- [162] M.B.B.J.M. Tuckerman, B. J. Berne, and G. J. Martyna. Reversible multiple time scale molecular dynamics. *The Journal of chemical physics*, 97(3):1990–2001, 1992.
- [163] J.C. Sexton and D.H. Weingarten. Hamiltonian evolution for the hybrid monte carlo algorithm. *Nuclear Physics B*, 380(3):665–677, 1992.
- [164] B. Shahbaba, S. Lan, W. O. Johnson, and R. M. Neal. Split hamiltonian monte carlo. *Statistics and Computing*, 24(3):339–349, 2014.
- [165] P. B. Mackenze. An improved hybrid monte carlo method. *Physics Letters B*, 226(3-4):369–371, 1989.
- [166] M. Betancourt. Identifying the optimal integration time in hamiltonian monte carlo. *arXiv preprint arXiv:1601.00225*, 2016.
- [167] Z. Wang, S. Mohamed, and N. Freitas. Adaptive hamiltonian and riemann manifold monte carlo. In *International conference on machine learning*, pages 1462–1470. PMLR, 2013.
- [168] A. Durmus, E. Moulines, and E. Saksman. On the convergence of hamiltonian monte carlo. *arXiv preprint arXiv:1705.00166*, 2017.
- [169] C. M. Campos and J. M. Sanz-Serna. Extra chance generalized hybrid monte carlo. *Journal of Computational Physics*, 281:365–374, 2015.
- [170] J. Sohl-Dickstein, M. Mudigonda, and M. DeWeese. Hamiltonian monte carlo without detailed balance. *International Conference on Machine Learning*, pages 719–726, 2014.
- [171] M. D. Hoffman, A. Gelman, et al. The no-u-turn sampler: adaptively setting path lengths in hamiltonian monte carlo. *J. Mach. Learn. Res.*, 15(1):1593–1623, 2014.
- [172] M. Ottobre, N. S. Pillai, F. J. Pinski, and A. M. Stuart. A function space hmc algorithm with second order langevin diffusion limit. *Bernoulli*, 22(1):60–106, 2016.
- [173] F. Heber, Z. Trst’ánová, and B. Leimkuhler. Posterior sampling strategies based on discretized stochastic differential equations for machine learning applications. *Journal of Machine Learning Research*, 21(228):1–33, 2020.
- [174] A. M. Horowitz. A generalized guided monte carlo algorithm. *Physics Letters B*, 268(2):247–252, 1991.
- [175] J. A. Izaguirre and S. S. Hampton. Shadow hybrid monte carlo: an efficient propagator in phase space of macromolecules. *Journal of Computational Physics*, 200(2):581–604, 2004.
- [176] T. Radivojević and E. Akhmatskaya. Modified hamiltonian monte carlo for bayesian inference. *Statistics and Computing*, 30(2):377–404, 2020.
- [177] H. Strathmann, D. Sejdinovic, S. Livingstone, Z. Szabo, and A. Gretton. Gradient-free hamiltonian monte carlo with efficient kernel exponential families. *arXiv preprint arXiv:1506.02564*, 2015.
- [178] C. Zhang, B. Shahbaba, and H. Zhao. Hamiltonian monte carlo acceleration using surrogate functions with random bases. *Statistics and computing*, 27(6):1473–1490, 2017.
- [179] T. Chen, E. Fox, and C. Guestrin. Stochastic gradient hamiltonian monte carlo. In *International conference on machine learning*, pages 1683–1691. PMLR, 2014.
- [180] M. Betancourt. The fundamental incompatibility of scalable hamiltonian monte carlo and naive data subsampling. In *International Conference on Machine Learning*, pages 533–540. PMLR, 2015.
- [181] A. Müller. Integral probability metrics and their generating classes of functions. *Advances in Applied Probability*, 29(2):429–443, 1997.
- [182] N. Aronszajn. Theory of reproducing kernels. *Transactions of the American mathematical society*, 68(3):337–404, 1950.
- [183] A. Berlinet and C. Thomas-Agnan. *Reproducing kernel Hilbert spaces in probability and statistics*. Springer Science & Business Media, 2011.
- [184] I. Steinwart and A. Christmann. *Support vector machines*. Springer Science & Business Media, 2008.

- [185] A. Barp, C.J. Simon-Gabriel, and L. Mackey. Targeted convergence characteristics of maximum mean discrepancies and kernel Stein discrepancies. *In preparation*.
- [186] B. K. Sriperumbudur, A. Gretton, K. Fukumizu, B. Schölkopf, and G. R.G. Lanckriet. Hilbert space embeddings and metrics on probability measures. *The Journal of Machine Learning Research*, 11:1517–1561, 2010.
- [187] K. Muandet, K. Fukumizu, B. Sriperumbudur, and B. Schölkopf. Kernel mean embedding of distributions: A review and beyond. *arXiv preprint arXiv:1605.09522*, 2016.
- [188] L. Schwartz. Sous-espaces hilbertiens d’espaces vectoriels topologiques et noyaux associés (noyaux reproduisants). *Journal d’analyse mathématique*, 13(1):115–256, 1964.
- [189] Carl-Johann Simon-Gabriel and Bernhard Schölkopf. Kernel distribution embeddings: Universal kernels, characteristic kernels and kernel metrics on distributions. *The Journal of Machine Learning Research*, 19(1):1708–1736, 2018.
- [190] B. K. Sriperumbudur, K. Fukumizu, and G. R.G. Lanckriet. Universality, characteristic kernels and rkhs embedding of measures. *Journal of Machine Learning Research*, 12(7), 2011.
- [191] C. Carmeli, E. De Vito, A. Toigo, and V. Umanitá. Vector valued reproducing kernel hilbert spaces and universality. *Analysis and Applications*, 8(01):19–61, 2010.
- [192] C.J. Simon-Gabriel, A. Barp, B. Schölkopf, and L. Mackey. Metrizing weak convergence with maximum mean discrepancies. *arXiv preprint arXiv:2006.09268*, 2020.
- [193] Stewart N Ethier and Thomas G Kurtz. *Markov processes: characterization and convergence*, volume 282. John Wiley & Sons, 2009.
- [194] Jackson Gorham and Lester Mackey. Measuring sample quality with kernels. In *International Conference on Machine Learning*, pages 1292–1301. PMLR, 2017.
- [195] C. Stein. A bound for the error in the normal approximation to the distribution of a sum of dependent random variables. In *Proceedings of the sixth Berkeley symposium on mathematical statistics and probability, volume 2: Probability theory*, volume 6, pages 583–603. University of California Press, 1972.
- [196] A. Anastasiou, A. Barp, F. Briol, B. Ebner, R. E. Gaunt, F. Ghaderinezhad, J. Gorham, A. Gretton, C. Ley, Q. Liu, et al. Stein’s method meets statistics: A review of some recent developments. *arXiv preprint arXiv:2105.03481*, 2021.
- [197] J. M. Lee. Smooth manifolds. In *Introduction to Smooth Manifolds*, pages 1–31. Springer, 2013.
- [198] C. Liu and J. Zhu. Riemannian stein variational gradient descent for bayesian inference. In *Proceedings of the AAAI Conference on Artificial Intelligence*, volume 32, 2018.
- [199] L. Hodgkinson, R. Salomone, and F. Roosta. The reproducing stein kernel approach for post-hoc corrected sampling. *arXiv preprint arXiv:2001.09266*, 2020.
- [200] A. D. Barbour. Stein’s method and poisson process convergence. *Journal of Applied Probability*, 25(A):175–184, 1988.
- [201] J. Gorham, A. B. Duncan, S. J Vollmer, and L. Mackey. Measuring sample quality with diffusions. *The Annals of Applied Probability*, 29(5):2884–2928, 2019.
- [202] Q. Liu and D. Wang. Stein variational gradient descent: A general purpose bayesian inference algorithm. *Advances in neural information processing systems*, 29, 2016.
- [203] C. J. Oates, M. Girolami, and N. Chopin. Control functionals for monte carlo integration. *Journal of the Royal Statistical Society: Series B (Statistical Methodology)*, 79(3):695–718, 2017.
- [204] A. Barp, F. Briol, . Duncan, M. Girolami, and L. Mackey. Minimum stein discrepancy estimators. In H. Wallach, H. Larochelle, A. Beygelzimer, F. d’Alché-Buc, E. Fox, and R. Garnett, editors, *Advances in Neural Information Processing Systems*, volume 32. Curran Associates, Inc., 2019.
- [205] W. Y. Chen, A. Barp, F. Briol, J. Gorham, M. Girolami, L Mackey, and C. Oates. Stein point markov chain monte carlo. In *International Conference on Machine Learning*, pages 1011–1021. PMLR, 2019.
- [206] K. Chwialkowski, H. Strathmann, and A. Gretton. A kernel test of goodness of fit. In *International conference on machine learning*, pages 2606–2615. PMLR, 2016.
- [207] Q. Liu, J. Lee, and M. Jordan. A kernelized stein discrepancy for goodness-of-fit tests. In *International conference on machine learning*, pages 276–284. PMLR, 2016.
- [208] A. Gretton, K. M. Borgwardt, M. J. Rasch, B. Schölkopf, and A. Smola. A kernel two-sample test. *The Journal of Machine Learning Research*, 13(1):723–773, 2012.
- [209] G. K. Dziugaite, D. M. Roy, and Z. Ghahramani. Training generative neural networks via maximum mean discrepancy optimization. *arXiv preprint arXiv:1505.03906*, 2015.
- [210] H. Park, S. Amari, and K. Fukumizu. Adaptive natural gradient learning algorithms for various stochastic models. *Neural Networks*, 13(7):755–764, 2000.
- [211] Y. Chen and W. Li. Natural gradient in wasserstein statistical manifold. *arXiv preprint arXiv:1805.08380*, 2018.
- [212] R. Karakida, M. Okada, and S. Amari. Adaptive natural gradient learning algorithms for unnormalized statistical models. In *International Conference on Artificial Neural Networks*, pages 427–434. Springer, 2016.

- [213] S. M. Kakade. A natural policy gradient. *Advances in neural information processing systems*, 14, 2001.
- [214] S. Bonnabel. Stochastic gradient descent on riemannian manifolds. *IEEE Transactions on Automatic Control*, 58(9):2217–2229, 2013.
- [215] M. Leok and J. Zhang. Connecting information geometry and geometric mechanics. *Entropy*, 19(10):518, 2017.
- [216] F. Briol, A. Barp, A. B. Duncan, and M. Girolami. Statistical inference for generative models with maximum mean discrepancy. 2019. arXiv:1906.05944.
- [217] A. Gretton, K. Fukumizu, Z. Harchaoui, and B. K. Sriperumbudur. A fast, consistent kernel two-sample test. In *NIPS*, volume 23, pages 673–681, 2009.
- [218] Damien Garreau, Wittawat Jitkrittum, and Motonobu Kanagawa. Large sample analysis of the median heuristic. *arXiv preprint arXiv:1707.07269*, 2017.
- [219] Danica J Sutherland, Hsiao-Yu Tung, Heiko Strathmann, Soumyajit De, Aaditya Ramdas, Alex Smola, and Arthur Gretton. Generative models and model criticism via optimized maximum mean discrepancy. *arXiv preprint arXiv:1611.04488*, 2016.
- [220] Aaditya Ramdas, Sashank J Reddi, Barnabas Poczos, Aarti Singh, and Larry Wasserman. Adaptivity and computation-statistics tradeoffs for kernel and distance based high dimensional two sample testing. *arXiv preprint arXiv:1508.00655*, 2015.
- [221] Chun-Liang Li, Wei-Cheng Chang, Yu Cheng, Yiming Yang, and Barnabás Póczos. Mmd gan: Towards deeper understanding of moment matching network. *arXiv preprint arXiv:1705.08584*, 2017.
- [222] K. Friston, J. Kilner, and L. Harrison. A free energy principle for the brain. *J. Physiology-Paris*, 100(1-3):70–87, 2006.
- [223] Thomas Parr. *The Computational Neurology of Active Vision*. PhD thesis, University College London, London, 2019.
- [224] Zafeirios Fountas, Noor Sajid, Pedro A. M. Mediano, and Karl Friston. Deep active inference agents using Monte-Carlo methods. *arXiv:2006.04176 [cs, q-bio, stat]*, June 2020.
- [225] Karl Friston, Conor Heins, Kai Ueltzhöffer, Lancelot Da Costa, and Thomas Parr. Stochastic Chaos and Markov Blankets. *Entropy*, 23(9):1220, September 2021.
- [226] Karl Friston, Lancelot Da Costa, Noor Sajid, Conor Heins, Kai Ueltzhöffer, Grigorios A. Pavliotis, and Thomas Parr. The free energy principle made simpler but not too simple. *arXiv:2201.06387 [cond-mat, physics:nlm, physics:physics, q-bio]*, January 2022.
- [227] Lancelot Da Costa, Karl Friston, Conor Heins, and Grigorios A. Pavliotis. Bayesian mechanics for stationary processes. *Proceedings of the Royal Society A: Mathematical, Physical and Engineering Sciences*, 477(2256):20210518, December 2021.
- [228] Karl Friston, Lancelot Da Costa, Danijar Hafner, Casper Hesp, and Thomas Parr. Sophisticated Inference. *Neural Computation*, 33(3):713–763, February 2021.
- [229] Thomas Parr, Lancelot Da Costa, Conor Heins, Maxwell James D. Ramstead, and Karl J. Friston. Memory and Markov Blankets. *Entropy*, 23(9):1105, September 2021.
- [230] Samuel Tenka. personal communication.
- [231] Philipp Schwartenbeck, Johannes Passecker, Tobias U Hauser, Thomas HB FitzGerald, Martin Kronbichler, and Karl J Friston. Computational mechanisms of curiosity and goal-directed exploration. *eLife*, page 45, 2019.
- [232] David M. Blei, Alp Kucukelbir, and Jon D. McAuliffe. Variational Inference: A Review for Statisticians. *Journal of the American Statistical Association*, 112(518):859–877, April 2017.
- [233] Daniel Kahneman and Amos Tversky. Prospect Theory: An Analysis of Decision under Risk. *Econometrica*, 47(2):263–291, 1979.
- [234] Sergey Levine. Reinforcement Learning and Control as Probabilistic Inference: Tutorial and Review. *arXiv:1805.00909 [cs, stat]*, May 2018.
- [235] Konrad Rawlik, Marc Toussaint, and Sethu Vijayakumar. On Stochastic Optimal Control and Reinforcement Learning by Approximate Inference. In *Twenty-Third International Joint Conference on Artificial Intelligence*, June 2013.
- [236] Marc Toussaint. Robot trajectory optimization using approximate inference. In *Proceedings of the 26th Annual International Conference on Machine Learning, ICML '09*, pages 1049–1056, Montreal, Quebec, Canada, June 2009. Association for Computing Machinery.
- [237] R. E. Kalman. A New Approach to Linear Filtering and Prediction Problems. *Journal of Basic Engineering*, 82(1):35–45, March 1960.
- [238] Emanuel Todorov. General duality between optimal control and estimation. In *2008 47th IEEE Conference on Decision and Control*, pages 4286–4292, December 2008.
- [239] Hilbert J. Kappen, Vicenç Gómez, and Manfred Opper. Optimal control as a graphical model inference problem. *Machine Learning*, 87(2):159–182, May 2012.
- [240] B. Ziebart. *Modeling Purposeful Adaptive Behavior with the Principle of Maximum Causal Entropy*. PhD thesis, Carnegie Mellon University, Pittsburgh, 2010.



- [241] E. T. Jaynes. Information Theory and Statistical Mechanics. *Physical Review*, 106(4):620–630, May 1957.
- [242] Andrzej Lasota and Michael C. MacKey. *Chaos, Fractals, and Noise: Stochastic Aspects of Dynamics*. Springer-Verlag, 1994.
- [243] David J. C. MacKay. *Information Theory, Inference and Learning Algorithms*. Cambridge University Press, Cambridge, UK ; New York, sixth printing 2007 edition edition, September 2003.
- [244] D. V. Lindley. On a Measure of the Information Provided by an Experiment. *The Annals of Mathematical Statistics*, 27(4):986–1005, 1956.
- [245] David J. C. MacKay. Information-Based Objective Functions for Active Data Selection. *Neural Computation*, 4(4):590–604, July 1992.
- [246] Pierre-Yves Oudeyer and Frederic Kaplan. What is Intrinsic Motivation? A Typology of Computational Approaches. *Frontiers in Neurobotics*, 1:6, November 2007.
- [247] Jürgen Schmidhuber. Formal Theory of Creativity, Fun, and Intrinsic Motivation (1990–2010). *IEEE Transactions on Autonomous Mental Development*, 2(3):230–247, September 2010.
- [248] A. Barto, M. Mirolli, and G. Baldassarre. Novelty or Surprise? *Frontiers in Psychology*, 4, 2013.
- [249] Yi Sun, Faustino Gomez, and Juergen Schmidhuber. Planning to Be Surprised: Optimal Bayesian Exploration in Dynamic Environments. *arXiv:1103.5708 [cs, stat]*, March 2011.
- [250] Edward Deci and Richard M. Ryan. *Intrinsic Motivation and Self-Determination in Human Behavior*. Perspectives in Social Psychology. Springer US, New York, 1985.
- [251] Laurent Itti and Pierre Baldi. Bayesian surprise attracts human attention. *Vision research*, 49(10):1295–1306, May 2009.
- [252] Thomas Parr, Noor Sajid, Lancelot Da Costa, M. Berk Mirza, and Karl J. Friston. Generative Models for Active Vision. *Frontiers in Neurobotics*, 15, 2021.
- [253] H. B. Barlow. *Possible Principles Underlying the Transformations of Sensory Messages*. The MIT Press, 1961.
- [254] R. Linsker. Perceptual Neural Organization: Some Approaches Based on Network Models and Information Theory. *Annual Review of Neuroscience*, 13(1):257–281, 1990.
- [255] L. M. Optican and B. J. Richmond. Temporal encoding of two-dimensional patterns by single units in primate inferior temporal cortex. III. Information theoretic analysis. *Journal of Neurophysiology*, 57(1):162–178, January 1987.
- [256] Richard E. Bellman. *Dynamic Programming*. Princeton University Press, Princeton, NJ, US, 1957.
- [257] K. J. Åström. Optimal control of Markov processes with incomplete state information. *Journal of Mathematical Analysis and Applications*, 10(1):174–205, February 1965.
- [258] Abraham Kaplan. *The Conduct of Inquiry*. Transaction Publishers, 1973.
- [259] Noor Sajid, Lancelot Da Costa, Thomas Parr, and Karl Friston. Active inference, Bayesian optimal design, and expected utility. *arXiv:2110.04074 [cs, math, stat]*, September 2021.
- [260] Oded Berger-Tal, Jonathan Nathan, Ehud Meron, and David Saltz. The Exploration-Exploitation Dilemma: A Multidisciplinary Framework. *PLOS ONE*, 9(4):e95693, April 2014.
- [261] Conor Heins, Beren Millidge, Daphne Demekas, Brennan Klein, Karl Friston, Iain Couzin, and Alexander Tschantz. Pymdp: A Python library for active inference in discrete state spaces. *arXiv:2201.03904 [cs, q-bio]*, January 2022.
- [262] Ryan Smith, Karl J. Friston, and Christopher J. Whyte. A step-by-step tutorial on active inference and its application to empirical data. *Journal of Mathematical Psychology*, 107:102632, April 2022.
- [263] Karl J. Friston, Marco Lin, Christopher D. Frith, Giovanni Pezzulo, J. Allan Hobson, and Sasha Ondobaka. Active Inference, Curiosity and Insight. *Neural Computation*, 29(10):2633–2683, October 2017.
- [264] Ozan Çatal, Tim Verbelen, Toon Van de Maele, Bart Dhoedt, and Adam Safron. Robot navigation as hierarchical active inference. *Neural Networks*, 142:192–204, October 2021.
- [265] Karl J. Friston, Richard Rosch, Thomas Parr, Cathy Price, and Howard Bowman. Deep temporal models and active inference. *Neuroscience & Biobehavioral Reviews*, 90:486–501, July 2018.
- [266] Christopher M. Bishop. *Pattern Recognition and Machine Learning*. Information Science and Statistics. Springer, New York, 2006.
- [267] Karl Friston, Thomas FitzGerald, Francesco Rigoli, Philipp Schwartenbeck, and Giovanni Pezzulo. Active Inference: A Process Theory. *Neural Computation*, 29(1):1–49, January 2017.
- [268] Karl Friston, Thomas FitzGerald, Francesco Rigoli, Philipp Schwartenbeck, John O’Doherty, and Giovanni Pezzulo. Active inference and learning. *Neuroscience & Biobehavioral Reviews*, 68:862–879, September 2016.
- [269] Ryan Smith, Philipp Schwartenbeck, Thomas Parr, and Karl J. Friston. An Active Inference Approach to Modeling Structure Learning: Concept Learning as an Example Case. *Frontiers in Computational Neuroscience*, 14, May 2020.
- [270] Karl Friston, Rosalyn J. Moran, Yukie Nagai, Tadahiro Taniguchi, Hiroaki Gomi, and Josh Tenenbaum. World model learning and inference. *Neural Networks*, 144:573–590, December 2021.

- [271] Samuel T Wauthier, Ozan Çatal, Tim Verbelen, and Bart Dhoedt. Sleep: Model Reduction in Deep Active Inference. page 13, 2020.
- [272] Alexander Tschantz, Anil K. Seth, and Christopher L. Buckley. Learning action-oriented models through active inference. *PLOS Computational Biology*, 16(4):e1007805, April 2020.
- [273] Karl Friston, Thomas Parr, and Peter Zeidman. Bayesian model reduction. *arXiv:1805.07092 [stat]*, October 2019.
- [274] Théophile Champion, Howard Bowman, and Marek Grześ. Branching Time Active Inference: Empirical study and complexity class analysis. *arXiv:2111.11276 [cs]*, November 2021.
- [275] Théophile Champion, Lancelot Da Costa, Howard Bowman, and Marek Grześ. Branching Time Active Inference: The theory and its generality. *arXiv:2111.11107 [cs]*, November 2021.
- [276] Domenico Maisto, Francesco Gregoretti, Karl Friston, and Giovanni Pezzulo. Active Tree Search in Large POMDPs. *arXiv:2103.13860 [cs, math, q-bio]*, March 2021.
- [277] Lancelot Da Costa, Noor Sajid, Thomas Parr, Karl Friston, and Ryan Smith. The relationship between dynamic programming and active inference: The discrete, finite-horizon case. *arXiv:2009.08111 [cs, math, q-bio]*, September 2020.
- [278] Aswin Paul, Lancelot Da Costa, Manoj Gopalkrishnan, and Adeel Razi. Active Inference for Stochastic and Adaptive Control in a Partially Observable Environment.
- [279] Cheng Zhang, Judith Butepage, Hedvig Kjellstrom, and Stephan Mandt. Advances in Variational Inference. *arXiv:1711.05597 [cs, stat]*, November 2017.
- [280] Thijs W. van de Laar and Bert de Vries. Simulating Active Inference Processes by Message Passing. *Frontiers in Robotics and AI*, 6, 2019.
- [281] Noor Sajid, Emma Holmes, Lancelot Da Costa, Cathy Price, and Karl Friston. A mixed generative model of auditory word repetition, January 2022.
- [282] Alexander Tschantz, Beren Millidge, Anil K. Seth, and Christopher L. Buckley. Control as Hybrid Inference. *arXiv:2007.05838 [cs, stat]*, July 2020.
- [283] John Winn and Christopher M Bishop. Variational Message Passing. *Journal of Machine Learning Research*, page 34, 2005.
- [284] M. J. Wainwright and M. I. Jordan. Graphical Models, Exponential Families, and Variational Inference. *Found. Trends in Mach. Learn.*, 1(1–2):1–305, 2007.
- [285] Thomas Parr, Dimitrije Markovic, Stefan J. Kiebel, and Karl J. Friston. Neuronal message passing using Mean-field, Bethe, and Marginal approximations. *Scientific Reports*, 9(1):1889, December 2019.
- [286] Sarah Schwöbel, Stefan Kiebel, and Dimitrije Marković. Active Inference, Belief Propagation, and the Bethe Approximation. *Neural Computation*, 30(9):2530–2567, September 2018.
- [287] Théophile Champion, Marek Grześ, and Howard Bowman. Realizing Active Inference in Variational Message Passing: The Outcome-Blind Certainty Seeker. *Neural Computation*, 33(10):2762–2826, September 2021.
- [288] Karl J. Friston, Thomas Parr, and Bert de Vries. The graphical brain: Belief propagation and active inference. *Network Neuroscience*, 1(4):381–414, December 2017.
- [289] Thomas Parr, Jakub Limanowski, Vishal Rawji, and Karl Friston. The computational neurology of movement under active inference. *Brain*, March 2021.